Impact of the 2011 Tohoku-oki Earthquake on the deep-sea benthos: Evidence from foraminifera of the Japan Trench slope

Akira Tsujimoto[1], Ritsuo Nomura[1], Kazuno Arai[2], Hidetaka Nomaki[3], Mutsuo Inoue[4], and Katsunori Fujikura[3]

[1]Faculty of Education, Shimane University, 1060 Nishikawatsucho, Matsue, Shimane 690-8504, Japan

[2]Center for Advanced Marine Core Research, Kochi University, B200 Monobe, Nankoku, Kochi 783-8502, Japan

[3]Japan Agency for Marine-Earth Science and Technology (JAMSTEC), 2-15 Natsushima-cho, Yokosuka, Kanagawa 237-0061, Japan

[4]Low Level Radioactivity Laboratory, Kanazawa University, Wake, Nomi, Ishikawa 923-1224, Japan

Correspondence to: A. Tsujimoto (tsujimoto@edu.shimane-u.ac.jp)

Abstract. We examined the impact of the 2011 Tohoku-oki earthquake and subsequent tsunami on the deep-sea benthic ecosystems based on sedimentological, radionuclide, and benthic foraminiferal analysis of core sediments, collected from 3200 and 3600 m water depths 5 and 17 months after the earthquake. Both sedimentological and radionuclide analysis of the excess ^{210}Pb, ^{134}Cs, and ^{137}Cs indicated that some of the analyzed sediment core recorded deposits before the earthquake, event deposits just after the earthquake, and deposits after the Fukushima Daiichi Nuclear Power Plant accident, which caused the release of a large amount of radioactive material 4 days after the earthquake. *Uvigerina senticosa*, *Chilostomella oolina*, and *Elphidium batialis* were the dominant species in the study area prior to the earthquake. In core 4W-2012, the pre-earthquake assemblage layer was covered by 5-cm-thick event deposits following the earthquake that contained a high diversity reworked foraminiferal assemblage. Following the episodic deposition, foraminiferal density drastically decreased and many species disappeared, resulting in a decrease in species diversity. After the disappearance of many benthic foraminiferal species, Opportunistic and competitive species gradually increased towards the sediment surface and became dominant in the top 1 cm of the core. Our results demonstrated that the episodic deposition resulting from the earthquake caused a drastic decrease in the original benthic foraminifera and colonization of opportunistic species with a low diversity within 17 months. Although there were differences in vertical profiles in the radionuclides and benthic foraminifera between sites, faunal change to the opportunistic species may have already occurred 5 months after the earthquake at this area.

1. Introduction

A powerful earthquake occurred off the Pacific coast of eastern Japan, on March 11, 2011, named as the 2011off the Pacific coast of Tohoku earthquake (hereafter the 2011 Tohoku-oki earthquake, Mw 9.0). The earthquake and subsequent tsunami caused seafloor disturbance in wide-ranging areas of the littoral zone, continental shelfs, continental slopes, and hadal zones (Arai et al., 2013; Oguri et al., 2013; Ikehara et al., 2014; Tamura et al., 2015). Some studies concerning the effect of the tsunami disturbances on the littoral benthic communities have been conducted (e.g., Seike et al., 2013; Urabe et al., 2013; Kanaya et al., 2015; Miura et al., 2017). These studies indicated that the immediate impact of the tsunami disturbances were changes in faunal composition, loss of species diversity, a reduction in the density, and an increase in the density of opportunistic taxa. The tsunami disturbances also affected benthic communities on the continental shelf and upper continental slope (Nomaki et al., 2016a). The mass sedimentation events must have affected the deep-sea ecosystems as was the case in the littoral and continental shelf ecosystems, but little is known regarding the impact, in particular deeper than 3000 m (e.g., Oguri et al., 2013; Kitahashi et al., 2014, 2016).

Benthic foraminifera (single-celled protists) are the most common eukaryotes in deep sea benthic communities, and they sometimes account for 50% or more of the eukaryotic biomass (Gooday et al., 1992; Nomaki et al., 2005). Their assemblages are influenced by various environmental factors, such as temperature, carbonate saturation state, oxygen concentration of the ambient water, and the quality and quantity of organic matter reaching the sediment surface (Murray, 2006; Jorissen et al., 2007 and references therein).

Foraminiferal calcite or agglutinated tests (shells) are abundantly preserved in sediment cores and can be used to reconstruct environmental changes in benthic communities. They have often been used as indicators of tsunami deposits mostly in shallow water areas based on their bathymetric distribution (Mamo et al., 2009 and references therein). Toyofuku et al. (2014) studied benthic foraminiferal communities at the continental shelf off Shimokita (northeast Japan) 5 months after the 2011 Tohoku-oki earthquake, and revealed that the communities were characterized by high species diversity and did not show a reduction in density, but an opportunistic fauna (*Psammosphaera* spp.) dominated the deeper site (211 m depth). While the shallow-water sediments preserve event deposits generated by both storms and earthquakes, which are difficult to separate (Tamura et al., 2015), off shore, deep-sea sediments are expected to have event deposits caused by earthquakes or subsequent tsunamis. Usami et al. (2017) studied benthic foraminiferal assemblages within turbidites collected from the upper slope sites off Sendai Bay (NE Japan) after the 2011 Tohoku-oki earthquake and concluded that benthic foraminiferal fauna can be a good indicator of turbidite paleoseismology. For precise reconstructions of paleoseismic events using sediment cores, it is essential to elucidate foraminiferal faunal changes before and after earthquakes, in particular in deep-sea environments.

In this study, we examined the sediment characteristics and foraminiferal assemblages in the four sediment cores collected from the landward slope of the Japan Trench around the hypocentral region 5 and 17 months after the earthquake. The event deposits caused by the earthquake and tsunami were determined using sedimentary facies and radionuclide analyses, namely ^{210}Pb, ^{134}Cs, and ^{137}Cs. Temporal changes in the foraminiferal assemblages and their diversities were examined through pre-earthquake sediment, event deposit, and post event sediments. This is the first record documenting the impact of large-scale seafloor disturbance on a deep-sea (deeper than 3000 m) benthic ecosystem using living and dead benthic foraminifera.

2. Materials and methods

2.1 Sampling procedure

Sediment core samples were collected using the human-occupied vehicle (HOV) *Shinkai 6500* during the YK11-E06 and the YK12-13 cruises of *R/V Yokosuka* in August 2011 and August 2012 (Fig. 1; Table 1). A push corer with an inner diameter of 8.2 cm was used to collect surface sediment (9 cm to 20 cm in length) at two different sites (2W: 38°39′N, 143°35′E, 3230 m water depth; 4W: 37°44′N, 143°17′E, ~3570 m water depth) for each cruise (i.e. both 2011 and 2012) (Table 1). Both sites were on a trench slope, but site 4W was along a small north-southward canyon (Fig. 1). Based on seismic reflection

profiles, both sites 2W and 4W are along topographic traces of fault systems; a buried normal fault at 2W and a landward dipping normal fault at 4W (Tsuji et al. 2013). Fissures on the seafloor and bacterial mats associated with mass deposition of megabenthos attributed to the 2011 Tohoku-oki earthquake were observed at 2W and 4W, respectively (Tsuji et al., 2013). To examine the effects of sediment disturbance on foraminiferal distributions and their recovery processes, our sediment cores were collected on 2011 and 2012 at normal seafloor, where no fissure and bacterial mat was nearby. The site 2W cores were collected ~300 m eastward from the fault scarp with a height of ~150 m (Fig 1B). The site 4W cores were collected at the canyon axes of a small north-southward canyon along the fault (Fig 1C). The 4W-2012 core was collected ~550 m south from 4W-2011 core, which resulted ~20 m differences in water depth (Fig. 1) due to limited dive time at the seafloor to perform various objectives of samplings (microbiological samplings, megabenthos samplings, geophysical measurement, geological observations, etc.).

On board, the overlying water was gently removed from the cores using a silicon tube. The sediment cores were subsampled into 0.5-cm-thick slices using a core extruder and then subdivided into two aliquots to separately analyze radionuclide and foraminiferal assemblage. The sliced sediments were stored at 4°C or -80°C for radionuclide and foraminiferal assemblage analyses, respectively.

2.2 Water and mud content analyses

In a laboratory on land, the sliced subsamples for radionuclide analysis were oven-dried at 50 ºC. Water contents were determined from the ratio of the wet and dry weights of the bulk sediments. Mud contents were determined based on the dry weights of the bulk samples calculated by the water content and the dry weight of the residues of the washed samples (>63-μm).

2.3 γ-Spectrometry

The oven-dried subsamples were pulverized to silt size using an agate mortar, after which 2 g of dry-weight sample was sealed in a styrene tube. The samples were left for more than three weeks to allow for radioactive secular equilibrium for ^{222}Rn and its daughter ^{214}Pb and ^{214}Bi with ^{226}Ra. Low-background γ-spectrometry was performed on the sediment samples using well-type Ge-detectors (Canberra EGPC150-P16; FWHM resolution 1.4 keV at 122 keV) for one counting day. For the calibration of ^{210}Pb and ^{214}Ra, we used the uranium standard issued from the New Brunswick Laboratory, USA (NBL-42-1). The excess of ^{210}Pb concentration was calculated by subtracting the weighted average of the 242, 295, and 352 keV of ^{214}Pb concentration from the total ^{210}Pb concentration (Irizuki et al., 2015).

We also calibrated the ^{134}Cs and ^{137}Cs concentrations in the sediment samples by comparing mock-up samples prepared using a reference material (JSAC0471) based on the γ-ray peaks of ^{134}Cs at 569 keV and 605 keV, and ^{137}Cs at 662 keV, respectively. The analytical precision for measuring ^{134}Cs was 7–38 %, based on the standard deviation of the counting statistics.

All concentration data in the present study were decay-corrected to the sampling date, and the ^{134}Cs/^{137}Cs ratio was decay-corrected to March 15, 2011, when major depositional events of radionuclides on land and the ocean surface occurred as a result of the Fukushima Daiichi Nuclear Power Plant accident.

2.4 Foraminiferal analysis

Thawed subsamples were wet-sieved through a 63-μm sieve. The residues of the depth intervals of the upper 10 cm were stained with Rose Bengal solution (1 g L^{-1}) for 24 h to distinguish live from dead individuals (Walton, 1952). The residues were oven-dried, and then dry-sieved through a 106-μm sieve (Nomura, 1995; Tsujimoto et al., 2013; Takata et al., 2015). Living specimens were identified by bright pink stained cytoplasm of at least few chambers (Schonfeld et al., 2013). Living

and dead specimens of the >106-μm fraction were dry-picked and analyzed. Sediment samples containing abundant foraminiferal specimens, i.e. upper part of 4W-2012 core (supplementary Table S1), were split into fractions containing approximately 200 specimens in total (i.e. living and dead). In other cases, all the foraminiferal specimens were picked up from the whole sediment sample (~12 ml for each layer). We also observed the siliceous biogenic particles (diatoms and radiolarians) of the >106-μm fraction under stereoscopic microscope while foraminiferal analysis. Foraminiferal density was calculated as number of individuals per gram of dry sediments, which calculated with wet weight of sample before the wet-sieving and water content data of the same horizon (see section 2.2).

We performed statistical analysis only for total assemblage of core 4W-2012 because the others did not contain sufficient numbers of specimens. We determined the Shannon Index (H') for the total (i.e. living and dead) assemblages containing more than 50 individuals using the PAST software package (version 3.16) (Krebs, 1989; Hammer and others, 2001). We also determined the rarefaction diversity E (S_{100}) (= the expected number of species in samples rarefied to 100 individuals). A Q-mode cluster analysis was also performed for total foraminiferal count data using the unweighted pair-group arithmetic average method of the PAST software package. The similarities used were Horn's overlap indices (Horn, 1966).

3. Results

3.1 Mud and water contents

Mud content varies in accordance with the changes in depositional condition. Generally, mud content becomes low under high-energy condition such as turbidite, and water content varies in accordance with the changes in mud content and sediment compaction after the deposition. Thus, mud and water content in sediment core become indicators for sedimentary environment. The mud and water contents were nearly stable throughout cores 4W-2011, 2W-2011, and 2W-2012 except for the water contents of the top cm of the cores (Fig. 2). Core 4W-2012 showed characteristic changes in mud and water contents throughout. The mud contents in core 4W-2012 were stable at approximately 90–95% from the bottom of the core (20 cm depth) to a depth of ca. 14 cm, but the values markedly decreased down to 54% and fluctuated between the ca. 14 to 9 cm depths (Fig. 2). The mud contents in core 4W-2012 became stable at approximately 95–100% from ca. 9 cm depth to the top of the core.

The water contents in core 4W-2012 were stable at approximately 70% from the bottom of the core (20 cm depth) to a depth of ca. 14 cm. Between ~14 cm to 9 cm depth, water contents fluctuated considerably, as seen as in the mud contents. The water contents in core 4W-2012 gradually increased from ca. 9 cm depth to the top of the core.

3.2 Vertical profiles of radionuclides

The excess ^{210}Pb concentrations in core 4W-2011 were quite low even at the surface and exponentially decreased downward, thus we analyzed only the top 4 cm of the core (Fig. 3). The excess ^{210}Pb concentrations in cores 2W-2011 and 2W-2012 were mostly stable throughout the cores of ~ 10cm length. In core 4W-2012, the excess ^{210}Pb concentrations were mostly stable down to 9 cm and then exhibited large fluctuations between 11 and 14 cm depth in sediments, followed by steep decrease at 15 cm depth. Although ^{134}Cs was detected only in the upper 1.5 cm in cores 2W-2011 and 2W-2012, ^{134}Cs was detected in the top 0–10 cm in core 4W-2012, and the two radiocesium isotopes exhibited the same trend (Fig. 4; Table 2). ^{134}Cs, which has a half-life of 2.1 years, was released into the environment by the Fukushima Daiichi Nuclear Power Plant (FNPP1) accident of March 11, 2011 (Mathieu et al., 2018). Major depositional events of radionuclides on land and the ocean surface occurred in particular from March 14–16 (Mathieu et al., 2018). The ratio of ^{134}Cs and ^{137}Cs, which indicates the origin of these radionuclides, are almost constant between sites and sediment depths.

3.3 Benthic foraminiferal assemblages

Scanning Electron Microscope (SEM) images of dominant and characteristic species are given in Figure S1. There

were few living (rose-Bengal stained) foraminifera and the total (living and dead) foraminiferal density decreased upward in core 4W-2011 (Fig. 5). Various species such as *Eilohedra rotunda*, *Elphidium batialis*, and *Pullenia bulloides* nearly disappeared above ca. 5 cm depth in the core, and *Uvigerina senticosa* above ca. 3 cm. Living foraminifera were found throughout the upper 10 cm of core 2W-2011 (Fig. 6). The dominant species were *Nonionella* spp., *Nonionellina labradorica*, *Brizalina pacifica*, and *Stainforthia* cf. *apertura* in order of their abundance (Fig. 6, Table S1). Living specimens of these species showed the highest density between ca. 1 to 4 cm depth in the core (Fig. 6). Although foraminiferal density was low in core 2W-2012, living specimens of *B. pacifica*, *N. labradorica*, and *Nonionella* spp. showed their highest density between ca. 0 to 2.5 cm depth in the core (Fig. 7). Whereas cores 4W-2011, 2W-2011, and 2W-2012 contained few foraminiferal tests (up to 28 ind. g^{-1} for total fauna), core 4W-2012 contained a relatively high number. Density of the dead foraminifera was low (ranging from 14 to 53 ind. g^{-1}) from the bottom of the core to ca. 13 cm, but it showed a spike peak (382 ind. g^{-1}) between ca. 12 to 9 cm (Fig. 8). The value decreased to a range from 4 to 12 individuals above ca. 9 cm depth except for the top of the core (Fig. 8). Living foraminifera were found throughout the upper 10 cm of the core, with the highest density at the sediment surface and a linear decrease down to ca. 5 cm depth in the core. The ratio of living foraminifera to total (living and dead) foraminifera (L/T ratio) increased from 10 cm to the upper part of the core, and reached a maximum (ca. 97%) at approximately 2 cm depth (Fig. 8).

Species diversity (H') and E (S_{100}) were measured to assess the temporal change in total foraminiferal biodiversity of core 4W-2012 (Fig. 8). Total diversity showed high values between ca. 14 to 9 cm depth, then decreased to the upper part of the core, and reached minimum values at approximately 4 cm depth. (Fig. 8).

Two major clusters (I, II) were distinguished for total foraminiferal assemblages based on the Q-mode cluster analysis for core 4W-2012 (Fig. S2). Vertical distributions of the absolute and relative abundances of the dominant foraminiferal species are shown with Q-mode cluster groupings in figure 9. Cluster I was divided into two sub-clusters (Ia and Ib) by the composition of the species. Sub-cluster Ia was characterized by the dominance of *Uvigerina senticosa* and *Chilostomella oolina*, with minor *Fursenkoina complanata*, *Brizalina pacifica*, and *Tosaia hanzawai*. Sub-cluster Ib was characterized by the dominance of *Nonionellina labradorica* and *Elphidium batialis*, with minor *F. complanata*, *B. pacifica*, and *T. hanzawai*. These species showed spike peaks between ca. 12 to 9 cm depth (Fig. 9). Cluster II was divided into three subclusters (IIa, IIb, and IIc) based on species composition. The densities were quite low in subcluster IIa, and this subcluster was characterized by the dominance of *E. batialis*, with minor *B. pacifica* (Fig. 9). Subcluster IIb was characterized by the dominance of *B. pacifica* and *Stainforthia* cf. *apertura*, with minor *E. batialis* and *N. labradorica*. Subcluster IIc was characterized by the dominance of *Stainforthia* cf. *apertura*, *N. labradorica*, and *Nonionella* spp., with minor *B. pacifica*. The species abundant in subcluster IIc were mostly living specimens (Fig. 9).

4. Discussion

4.1 Sea floor disturbance resulting from the 2011 Tohoku-oki Earthquake and the influx of ^{134}Cs and ^{137}Cs

^{210}Pb has a half-life of 22.3 years and has been used to estimate depositional ages up to a maximum of ca. 150 years, i.e. up to 7 half-lives (Lowe and Walker, 2014). ^{137}Cs is an artificial radionuclide, and has been detected in sediments from 1954 onwards, with a maximum in 1963 because of intensive releases from aerial nuclear tests (Lowe and Walker, 2014). ^{134}Cs was released into the environment after the Fukushima Daiichi Nuclear Power Plant (FNPP1) accident, and the first major releases occurred on March 15 (Mathieu et al., 2018). These radionuclides, particularly short-lived ^{134}Cs (2.06 years), have been used to distinguish post-sediment from pre-sediment of the 2011 Tohoku-oki Earthquake (Oguri et al., 2013; Toyofuku et al., 2014; Ikehara et al., 2014, 2016).

The very low ^{210}Pb concentrations in core 4W-2011 suggest that the surface sediments at this site were eroded prior to the sampling. Although cores 4W-2011 and 4W-2012 were collected in the same area, slight locational changes in the canyon may result in different sedimentation environments; 4W-2011 was collected from a steeper slope (~4°) while 4W-2012 was

collected from a gentle slope (~1°) of the same canyon on the basis of the bathymetric profile along the two sites (Fig. S3). Sedimentation rates can vary greatly even at local scale, in particular at such topographic and hydrographic heterogeneity environments. Indeed, many dead megafauna and debris were accumulated just southeast from the 4W-2012 sites while they were minor at the north side including 4W-2011 sites. A flow such as a turbidity current was accelerated by an increase in slope gradient and eroded the surface sediment near 4W-2011. The flow was decelerated by a decrease in the slope gradient and deposited the new turbidite near 4W-2012. As the consequence, the lithology and profiles of radionuclides between the two cores are quite different.

^{210}Pb concentrations in cores 2W-2011 and 2W-2012 indicate intense sediment mixing and/or a high sedimentation rate. In core 4W-2012, the low concentrations of the excess ^{210}Pb below 15 cm depth indicate that these sediments are sufficiently old. Moreover, the sharp increase of the excess ^{210}Pb concentrations at approximately 15 cm depth towards surface indicates that there is a sedimentation gap at this depth. This is confirmed by the markedly decreased mud contents and fluctuation above ca. 14 cm depth (Fig. 2). X-ray CT image of the core collected few meters away from our4W-2012 core clearly indicates event deposits layers comparable with our analyzed core (Fig. S4). Laminated layer between ca. 11 to 5 cm depth in the image of 4W site-2012 is interpreted as turbidite, which is comparable to 15 to 9 cm depth in 4W-2012 core. These results and the fluctuation of the excess ^{210}Pb between 15 cm to 9 cm, combined with the lack of detectable ^{134}Cs in this interval, suggest that these sediments facies are event deposits that were deposited immediately after the 2011 Tohoku-oki Earthquake.

^{134}Cs was detected in the top 0–1.5 cm of cores 2W-2011 and 2W-2012, and the top 0–9.5 cm of core 4W-2012 (Fig. 4 and Table 2). Because of its short half-life (2.06 y) and comparable ^{134}Cs/^{137}Cs ratios (0.85 to 1.12, average; 0.95) (Fig. 4 and Table 2) between those released from the FNPP1 (approximately 1: Komori et al., 2013; Kobayashi et al., 2015, 2017), ^{134}Cs detected in the sediment samples was derived entirely from the FNPP1 accident. Honda et al. (2013) analyzed timeseries sinking particles in sediment traps deployed 950 km southeast from the FNPP1 before and after the FNPP1 accident, which caused major deposition of radionuclides on land and the ocean surface from March 14–16. They reported that ^{134}Cs and ^{137}Cs from the FNPP1 accident were detected in sinking particles collected at 500 m after late March 2011 and at 4810 m after early April 2011. Oguri et al. (2013) detected ^{134}Cs in a sediment core collected at a water depth of 7261 m in the Japan Trench. They suggested that diatom blooms accelerated rapid deposition of ^{134}Cs in the hadal environment. The Kuroshio-Oyashio Transition zone is situated in the northwest Pacific Ocean, where the mixing of cold nutrient-rich Oyashio waters and warm oligotrophic Kuroshio waters occurs (Inagake and Saitoh, 1998; Itoh and Sugimoto, 2002). In the Kuroshio-Oyashio Transition zone, a spring bloom of primary production occurs because of eddy-driven nutrient fluxes (Inagake and Saitoh, 1998; Sasai et al., 2007; Sasai et al., 2010). The spring bloom is mainly composed of diatoms (Isada et al., 2009; Yatsu et al., 2013), and a large influx of diatoms is deposited on the seafloor (Ikehara et al., 2016). Otosaka et al. (2014) studied time-series sinking particles from August, 2011 to June, 2013 at about 100 km east of the FNPP1. They reported that the production of diatoms and subsequent sinking of biogenic particles caused the increase in total mass flux of sinking particles from April to June. They concluded that adsorption or incorporation of radiocesium onto particles in the surface water and following rapid sinking of particles are considered as primary mechanisms of accumulation of radiocesium on the seafloor. Although radiolarians were dominant in the >106-μm fraction in the lower part of core 4W-2012based on microscopic qualitative observations, diatoms became dominant in the upper part (above ca. 9 cm depth) (Fig S5). The gradual decrease in water content with increasing sediment depth suggests continuous sedimentation and compactions of diatoms in this interval. Thus, we concluded that the sediments of the upper 10 cm of core 4W-2012 were deposited from March 2011 to August 2012 (within 17 months), probably related to the mass bloom of the phytoplankton. Although a sedimentation rate of ~6 cm per year is quite high, similar rapid sedimentation rates have sometimes been reported in depositional environments such as submarine canyons or trenches (Oguri et al., 2013). Cores 2W-2011 and 2W-2012 were collected at the same site with approximately 1 year interval. Detection of ^{134}Cs in the top 0–1.5 cm of both cores may indicate mass sedimentation did not occur from August 2011 to August 2012 at this site. Differences in vertical change in radionuclides between the sites may indicate that sedimentary and erosional

processes were different because of differences in surface productivity or topography, such as the small canyons observed at 4W (Fig 1 and Fig S3).

Based on these observations, we divided the sediments of core 4W-2012 into three facies as follows: FI) deposits before the earthquake (20–15 cm depth), FII) event deposits immediately after the earthquake (15–9 cm depth), and FIII) deposits after the FNPP1 accident (above 9 cm depth) based on the changes in radionuclides. We discuss the benthic foraminiferal faunal change of the deep-sea floor disturbance focusing on the data of core 4W-2012 because the others do not contain sufficient specimens and are not appropriate for detailed discussion.

4.2 Benthic foraminiferal faunal change by the deep-sea floor disturbance

In this study, we followed the procedure for rose-Bengal staining method by Takayanagi (1978) and subsequent studies (e.g., Tsujimoto et al., 2006; Nomura and Kawano, 2011). This procedure is different from recent ecological or environmental monitoring studies using benthic foraminifera (e.g., Schönfeld et al., 2012). Because the living assemblage may be underrepresented by our procedure due to short staining time and staining after freeze-thawing, our discussion is mainly based on total fauna, not by "living" fauna. Furthermore, analyzed size fraction (>106-μm) was follows our conventional procedure by Nomura (1995), Tsujimoto et al. (2013), and Takata et al. (2015), which studied deep sea benthic foraminifera. Most ecological studies used either 63 μm or 125μm sieves, and the differences in sieve size in our studies hampers direct comparison with such ecological or environmental monitoring studies. Although these limitations on staining and sieve-sizes, temporal trend in total foraminiferal assemblage in our study clearly showed the impact of large-scale seafloor disturbance on deep-sea benthic ecosystem together with concurrent sedimentological analyses.

Changes in benthic foraminiferal assemblages of core 4W-2012 coincide with three sediment facies based on sedimentological and radionuclides analyses (facies FI, FII, and FIII, which correspond pre-earthquake deposits, event deposits immediately after the earthquake, and deposits after the FNPP1 accident, respectively). Cluster Ia of the benthic foraminifera is equivalent to sediment facies FI, pre-earthquake sediments. The dominant and characteristic species of cluster Ia were *Uvigerina senticosa* and *Chilostomella oolina*. Thompson (1980) reported the bathymetric distributions of dominant benthic foraminiferal species in the Japan Trench area using sediment samples from Deep Sea Drilling Program Leg56 sites and Lamont Doherty Geological Observatory core collections (Fig. 10). Although the main study area of Thompson (1980) was the northern part of the Japan Trench area (Fig. 1), *U. senticosa* was the dominant species at the approximate water depth of our study site (3585 m) (Fig. 10). *Chilostomella oolina* is not documented at an approximate water depth of 3500 m in Thompson (1980), but this species is reported as a characteristic species at depths greater than 3000 m in different areas (Schmiedl and Mackensen, 1997; Uchimura et al., 2017). The most dominant foraminiferal species below 5 cm in core 4W-2011 is also *U. senticosa* (Fig. 5), and this interval is sufficiently old (>150 years) based on the ^{210}Pb profile. Thus, cluster Ia of core 4W-2012 indicates an assemblage before the effects of the earthquake.

Cluster Ib of benthic foraminifera is equivalent to the sediment facies FII event deposits immediately following the earthquake. *Uvigerina senticosa* and *C. oolina*, which are the dominant species in cluster Ia, gradually decrease and nearly disappear at the top of the cluster Ib. Instead, *Nonionellina labradorica* and *Elphidium batialis* become dominant towards the top of cluster Ib. Many other species were found in this facies, resulting in high species diversity (Fig. 8). These species in general distribute at water depths of 1800–3400 m (Fig. 10; Thompson, 1980). *Bolivina spissa*, nearly only found from cluster Ib, has been reported in the oxygen minimum zone of the Pacific Ocean (Ingle et al., 1980; Quinterno and Gardner, 1987; Fontanier et al., 2014). Fontanier et al. (2014) studied living benthic foraminiferal assemblages between 500–2000 m depth off Hachinohe (northeast Japan). They reported that the *B. spissa* distribution is restricted to stations bathed by dysoxic waters between 760–1250 m depth. This species is reported from shallower than a water depth of 2319 m in the Japan Trench area (Fig. 10; Thompson, 1980), thus sediment reworking at shallower water depths by an episodic event and subsequent sedimentation of reworked particles may have occurred following the earthquake.

Cluster II of the benthic foraminifera is equivalent to sediment facies FIII, the diatom ooze sediment deposited following the Fukushima-Daiichi Nuclear Power plant accident. The foraminiferal density drastically decreased in cluster I and many species of cluster I disappeared in subcluster IIa (9–7 cm depth), resulting in a decrease in species diversity. *Brizalina pacifica* and *Stainforthia* cf. *apertura* appeared in subcluster IIb (7–4 cm depth), then *S.* cf. *apertura*, *Nonionella* spp. (mainly composed of *N. globosa*), and *N. labradorica* became dominant in subcluster IIc (4–0 cm depth). Most these species are composed of rose-Bengal stained specimens and found to be dominant at the surface 1 or 2 cm.

In sum, the episodic deposition related to the earthquake resulted in a drastic faunal change in the pre-earthquake benthic foraminifera, and a new assemblage with low diversity was established. Similar low diversity assemblages influenced by the deposition of turbidities have been reported in upper continental slope and deep-sea canyons (Hess et al., 2005; Hess and Jorissen, 2009; Toyofuku et al., 2014; Bolliet et al., 2014). These studies showed that opportunistic taxa colonized and rapidly flourished after the disturbance of the seafloor. Kitazato et al. (2000) monitored the response of benthic foraminifera to seasonal inputs of organic matter from phytoplankton in Sagami Bay, Japan, and showed that the density of *Brizalina pacifica* (reported as *Bolivina pacifica* in their study) and *S. apertura* rapidly increased in response to the spring bloom at the ocean surface. A spring bloom of phytoplankton was observed between late March and early April 2011 off the Tohoku area, and depositions of phytodetritus aggregations were confirmed along the Japan Trench slope (Oguri et al., 2013). Indeed, very high total organic carbon (TOC) concentrations were recorded in the sediment core collected from ~10s cm away from our foraminiferal core 4W-2012. The TOC concentrations were approximately 4.5% in the surface 2 cm, and >4% even at the 10 cm depth in sediments (Table S2). Almost constant values of C/N ratios, carbon and nitrogen isotopic compositions through the 10 cm depth (Table S2) suggest almost same origin of these high quantity of organic matters. These high TOC concentrations down to 10 cm suggest rapid burial of organic matter before its mineralization, which coincide to the rapid sedimentation events down to 13 cm suggested by ^{210}Pb profiles (Fig. 3). Thus, rapid deposition of phytoplankton may have enhanced the flourishing of these opportunistic taxa during the 17 months following the earthquake. *Nonionella globosa* is a shallow-to-deep infauna and *N. labradorica* is an intermediate-to-deep infauna (Fontanier et al., 2014). These species are putatively deposit feeders, and more competitive than others (Fontanier et al., 2014), thus these species also could flourish in the top of the core. Although the abundances were low, these species were also found in cores 2W-2011 and 2W-2012 as dominant species (Figs. 6 and 7). The vertical distribution pattern showing increases above 5 cm is similar among the three cores. Thus, faunal change may have already occurred 5 months after the earthquake. Hess et al. (2005) reported that the recovery of benthic foraminiferal assemblages by the turbidite deposition was in the 1.5 year, and the community structure was in an early stage of recolonization. In our present study, some species belonging to cluster Ia (pre-earthquake) were also found from the sediment surface (e.g., *Fursenkoina complanata*), suggesting an early recovery stage of original assemblages. However, it may take a much longer time to recover original assemblages because the disturbance at the 4W sites might have been more severe than Hess et al. (2005).

5. Conclusions

In this study, we examined the sediment characteristics and foraminiferal assemblages in the sediment cores collected from the landward slope of the Japan Trench around the hypocentral region 5 and 17 months after the 2011 Tohoku-oki earthquake (Mw 9.0) to document the impact of large-scale seafloor disturbance on a deep-sea benthic ecosystem.

^{134}Cs from the Fukushima Daiichi Nuclear Power Plant accident was detected in three of the four examined cores. In particular, ^{134}Cs was detected in the top 0–10 cm of core 4W-2012, collected at the 4W site. The core was collected in August 2012, thus the sedimentation rate was estimated as 6 cm/year. This high sedimentation rate is probably related to the mass bloom of phytoplankton and the canyon topography where sediments are eroded/deposited.

We found a benthic foraminiferal faunal change related to the deep-sea floor disturbance in the landward slope of

the Japan Trench as follows.

The “original” assemblage, consisting of *Uvigerina senticosa*, *Chilostomella oolina*, and *Elphidium batialis*, was covered by sediment with a high diversity reworked assemblage related to event deposits following the earthquake. After the episodic deposition, the density drastically decreased and many species disappeared, resulting in a decrease in species diversity. Opportunistic species, such as *Brizalina pacifica* and *Stainforthia* cf. *apertura*, and competitive species, such as *Nonionella* spp. and *N. labradorica*, gradually increased toward the sediment surface and became dominant in the top of the core. These faunal changes may have already occurred 5 months after the earthquake, and rapid deposition of phytoplankton may have enhanced the flourishing of these opportunistic taxa in the high sedimentation area. Further study will show the long-term recovery process of this deep-sea benthic ecosystem following mass disturbance of the seafloor.

Acknowledgements

We would like to thank the crews and scientists of the *R/V Yokosuka* and the *HOV Shinkai 6500* of the Japan Agency for Marine–Earth Science and Technology (JAMSTEC) during the YK11-E06 and YK12-13 cruises; Dr. Wataru Tanikawa for X-ray CT measurement. Reviews by two anonymous reviewers greatly improved the manuscript. This study was financially supported by the research project Tohoku Ecosystem-Associated Marine Sciences from the Ministry of Education, Culture, Sports, Science, and Technology. This study was partially performed under the cooperative research program of Center for Advanced Marine Core Research, Kochi University (12A005, 12B004).

References

Arai, K., Naruse, H., Miura, R., Kawamura, K., Hino, R., Ito, Y., Inazu, D., Yokokawa, M., Izumi, N., Murayama, M. and Kasaya, T.: Tsunami-generated turbidity current of the 2011 Tohoku-Oki earthquake, Geology, 41(11), 1195–1198, doi:10.1130/G34777.1, 2013.

Bolliet, T., Jorissen, F. J., Schmidt, S. and Howa, H.: Benthic foraminifera from Capbreton Canyon revisited; faunal evolution after repetitive sediment disturbance, Deep. Res. Part II, 104, 319–334, doi:10.1016/j.dsr2.2013.09.009, 2014.

Fontanier, C., Duros, P., Toyofuku, T., Oguri, K., Koho, K. A., Buscail, R., Gremare, A., Radakovitch, O., Deflandre, B., De Nooijer, L. J., Bichon, S., Goubet, S., Ivanovsky, A., Chabaud, G., Menniti, C., Reichart, G.-J. and Kitazato, H.: Living (Stained) Deep-Sea Foraminifera off Hachinohe (NE Japan, Western Pacific): Environmental Interplay in Oxygen-Depleted Ecosystems, J. Foraminifer. Res., 44(3), 281–299, doi:10.2113/gsjfr.44.3.281, 2014.

Gooday, A. J., Levin, L. A., Linke, P., and Heeger, T.: The role of benthic foraminifera in deep-sea food webs and carbon cycling, in G. T Rowe, and V. Pariente eds., Deep-sea food chains and the global carbon cycle, 63–91, Kluwer Academic Publishers, Netherlands, 1992.

Hammer, Ø., Harper, D. A. T. a. T. and Ryan, P. D.: PAST: Paleontological Statistics Software Package for Education and Data Analysis, Palaeontol. Electron., 4(1), 1–9, doi:10.1016/j.bcp.2008.05.025, 2001.

Hess, S. and Jorissen, F. J.: Distribution patterns of living benthic foraminifera from Cape Breton canyon, Bay of Biscay: Faunal response to sediment instability, Deep. Res. Part I Oceanogr. Res. Pap., 56(9), 1555–1578, doi:10.1016/j.dsr.2009.04.003, 2009.

Hess, S., Jorissen, F. J., Venet, V. and Abu-Zied, R.: Benthic Foraminiferal Recovery After Recent Turbidite Deposition in Cap Breton Canyon, Bay of Biscay, J. Foraminifer. Res., 35(2), 114–129, doi:10.2113/35.2.114, 2005.

Honda, M. C., Kawakami, H., Watanabe, S. and Saino, T.: Concentration and vertical flux of Fukushima-derived radiocesium in sinking particles from two sites in the Northwestern Pacific Ocean, Biogeosciences, 10(6), 3525–3534, doi:10.5194/bg-10-3525-2013, 2013.

Horn, H. S.: Measurement of "Overlap" in Comparative Ecological Studies, Am. Nat., 100(914), 419–424, doi:10.1086/282436, 1966.

Ikehara, K., Irino, T., Usami, K., Jenkins, R., Omura, A. and Ashi, J.: Possible submarine tsunami deposits on the outer shelf of Sendai Bay, Japan resulting from the 2011 earthquake and tsunami off the Pacific coast of Tohoku, Mar. Geol., 358, 120–127, doi:10.1016/j.margeo.2014.11.004, 2014.

Ikehara, K., Kanamatsu, T., Nagahashi, Y., Strasser, M., Fink, H., Usami, K., Irino, T. and Wefer, G.: Documenting large earthquakes similar to the 2011 Tohoku-oki earthquake from sediments deposited in the Japan Trench over the past 1500 years, Earth Planet. Sci. Lett., 445, 48–56, doi:10.1016/j.epsl.2016.04.009, 2016.

Inagake, D. and Saitoh, S.: Description of the oceanographic condition off Sanriku, northwestern Pacific, and its relation to spring bloom detected by the Ocean Color and Temperature Scanner (OCTS) images, J. Oceanogr., 54(1987), 479–494, doi:10.1007/BF02742450, 1998.

Ingle, J. C., Keller, G., Kolpack, R. L. and Kolpack, R. L.: Benthic Foraminiferal Biofacies, Sediments and Water Masses of the Southern Peru-Chile Trench Area, Southeastern Pacific Ocean, Micropaleontology, 26(2), 113, doi:10.2307/1485435, 1980.

Irizuki, T., Ito, H., Sako, M., Yoshioka, K., Kawano, S., Nomura, R. and Tanaka, Y.: Anthropogenic impacts on meiobenthic Ostracoda (Crustacea) in the moderately polluted Kasado Bay, Seto Inland Sea, Japan, over the past 70 years, Mar. Pollut. Bull., 91(1), 149–159, doi:10.1016/J.MARPOLBUL.2014.12.013, 2015.

Isada, T., Kuwata, A., Saito, H., Ono, T., Ishii, M., Yoshikawa-Inoue, H. and Suzuki, K.: Photosynthetic features and primary productivity of phytoplankton in the Oyashio and Kuroshio-Oyashio transition regions of the northwest Pacific, J. Plankton Res., 31(9), 1009–1025, doi:10.1093/plankt/fbp050, 2009.

Itoh, S. and Sugimoto, T.: Direct current measurements off Sanriku, east of Japan, J. Oceanogr., 58(6), doi:10.1023/A:1022883415672, 2002.

Jorissen, F. J., Fontanier, C. and Thomas, E.: Chapter Seven Paleoceanographical Proxies Based on Deep-Sea Benthic Foraminiferal Assemblage Characteristics, Dev. Mar. Geol., 1, 263–325, doi:10.1016/S1572-5480(07)01012-3, 2007.

Kanaya, G., Suzuki, T. and Kikuchi, E.: Impacts of the 2011 tsunami on sediment characteristics and macrozoobenthic assemblages in a shallow eutrophic lagoon, Sendai Bay, Japan, PLoS One, 10(8), 1–18, doi:10.1371/journal.pone.0135125, 2015.

Kitahashi, T., Jenkins, R. G., Nomaki, H., Shimanaga, M., Fujikura, K. and Kojima, S.: Effect of the 2011 Tohoku Earthquake on deep-sea meiofaunal assemblages inhabiting the landward slope of the Japan Trench, Mar. Geol., 358, 128–137, doi:10.1016/j.margeo.2014.05.004, 2014.

Kitahashi, T., Watanabe, H., Ikehara, K., Jenkins, R. G., Kojima, S. and Shimanaga, M.: Deep-sea meiofauna off the Pacific coast of Tohoku and other trench slopes around Japan: a comparative study before and after the 2011 off the Pacific coast of Tohoku Earthquake, J. Oceanogr., 72(1), 129–139, doi:10.1007/s10872-015-0323-3, 2016.

Kitazato, H., Shirayama, Y., Nakatsuka, T., Fujiwara, S., Shimanaga, M., Kato, Y., Okada, Y., Kanda, J., Yamaoka, A., Masuzawa, T. and Suzuki, K.: Seasonal phytodetritus deposition and responses of bathyal benthic foraminiferal populations in Sagami Bay, Japan: Preliminary results from "Project Sagami 1996-1999," Mar. Micropaleontol., 40(3), 135–149, doi:10.1016/S0377-8398(00)00036-0, 2000.

Kobayashi, S., Shinomiya, T., Ishikawa, T., Imaseki, H., Iwaoka, K., Kitamura, H., Kodaira, S., Kobayashi, K., Oikawa, M., Miyaushiro, N., Takashima, Y. and Uchihori, Y.: Low134Cs/137Cs ratio anomaly in the north-northwest direction from the Fukushima Dai-ichi Nuclear Power Station, J. Environ. Radioact., 178–179, 84–94, doi:10.1016/j.jenvrad.2017.07.023, 2017.

Kobayashi, S., Shinomiya, T., Kitamura, H., Ishikawa, T., Imaseki, H., Oikawa, M., Kodaira, S., Miyaushiro, N., Takashima, Y. and Uchihori, Y.: Radioactive contamination mapping of northeastern and eastern Japan by a car-borne survey system, Radi-Probe, J. Environ. Radioact., 139, 281–293, doi:10.1016/j.jenvrad.2014.07.026, 2015.

Komori, M., Shozugawa, K., Nogawa, N. and Matsuo, M.: Evaluation of Radioactive Contamination Caused by Each Plant of Fukushima Daiichi Nuclear Power Station Using $^{134}Cs/^{137}Cs$ Activity Ratio as an Index, Bunseki Kagaku, 62(6), 475–483, doi:10.2116/bunsekikagaku.62.475, 2013.

Krebs, C. J.: Ecological Methodology: Harper and Row Publishers, New York, 654 p., 1989.

Lowe, J.J. and Walker, M.J.C.: Reconstructing Quaternary Environments. third ed. Routledge, London., 2014

Mamo, B., Strotz, L. and Dominey-howes, D.: Earth-Science Reviews Tsunami sediments and their foraminiferal assemblages, Earth Sci. Rev., 96(4), 263–278, doi:10.1016/j.earscirev.2009.06.007, 2009.

Mathieu, A., Kajino, M., Korsakissok, I., Périllat, R., Quélo, D., Quérel, A., Saunier, O., Sekiyama, T. T., Igarashi, Y. and Didier, D.: Fukushima Daiichi–derived radionuclides in the atmosphere, transport and deposition in Japan: A review, Appl. Geochemistry, 91(June 2017), 122–139, doi:10.1016/j.apgeochem.2018.01.002, 2018.

Miura, O., Kanaya, G., Nakai, S., Itoh, H., Chiba, S., Makino, W., Nishimura, T., Kojima, S. and Urabe, J.: Ecological and genetic impact of the 2011 Tohoku Earthquake Tsunami on intertidal mud snails, Sci. Rep., 7(September 2016), 1–10, doi:10.1038/srep44375, 2017.

Murray, J. W.: Ecology and applications of benthic foraminifera, Cambridge University Press., 2006.

Nomaki, H., Heinz, P., Nakatsuka, T., Shimanaga, M., and Kitazato, H. Species-specific ingestion of organic carbon by deep

sea benthic foraminifera and meiobenthos: In situ tracer experiments. Limnol. Oceanogr., 50, 134–146, doi:10.4319/lo.2005.50.1.0134, 2005.

Nomaki, H., Mochizuki, T., Kitahashi, T., Nunoura, T., Arai, K., Toyofuku, T., Tanaka, G., Shigeno, S., Tasumi, E., Fujikura, K. and Watanabe, S.: Effects of mass sedimentation events after the 2011 off the Pacific coast of Tohoku Earthquake on benthic prokaryotes and meiofauna inhabiting the upper bathyal sediments, J. Oceanogr., 72(1), 113–128, doi:10.1007/s10872-015-0293-5, 2016a.

Nomaki, H., Arai, K., Suga, H., Toyofuku, T., Wakita, M., Nunoura, T., Oguri, K., Kasaya, T. and Watanabe, S.: Sedimentary organic matter contents and porewater chemistry at upper bathyal depths influenced by the 2011 off the Pacific coast of Tohoku Earthquake and tsunami, J. Oceanogr., 72(1), 99–111, doi:10.1007/s10872-015-0315-3, 2016b.

Nomura, R.: Paleogene to Neogene Deep-Sea Paleoceanography in the Eastern Indian Ocean: Benthic Foraminifera from ODP Sites 747, 757 and 758, Micropaleontology, 41(3), 251, doi:10.2307/1485862, 1995.

Nomura, R. and Kawano, S.: Foraminiferal assemblages response to anthropogenic influence and parallel to decadal sea-level changes over the last 70 years in Lake Kugushi , Fukui Prefecture , southwest Japan, Quat. Int., 230(1–2), 44–56, doi:10.1016/j.quaint.2010.01.011, 2011.

Oguri, K., Kawamura, K., Sakaguchi, A., Toyofuku, T., Kasaya, T., Murayama, M., Fujikura, K., Glud, R. N. and Kitazato, H.: Hadal disturbance in the Japan Trench induced by the 2011 Tohoku-Oki earthquake, Sci. Rep., 3, 1–6, doi:10.1038/srep01915, 2013.

Otosaka, S., Nakanishi, T., Suzuki, T., Satoh, Y. and Narita, H.: Vertical and lateral transport of particulate radiocesium off fukushima, Environ. Sci. Technol., 48(21), 12595–12602, doi:10.1021/es503736d, 2014.

Quinterno, P. J. and Gardner, J. V.: Benthic foraminifers on the continental shelf and upper slope, Russian River area, Northern California, J. Foraminifer. Res., 17(2), 132–152, doi:10.2113/gsjfr.17.2.132, 1987.

Sasai, Y., Sasaoka, K., Sakaki, H. and Ishida, A.: Seasonal and intra-seasonal variability of chlorophyll-a in the North Pacific: model and satellite data, J. Earth Simulator, 8(November), 3–11, 2007.

Sasai, Y., Richards, K. J., Ishida, A. and Sasaki, H.: Effects of cyclonic mesoscale eddies on the marine ecosystem in the Kuroshio Extension region using an eddy-resolving coupled physical-biological model, Ocean Dyn., 60(3), 693–704, doi:10.1007/s10236-010-0264-8, 2010.

Schmiedl, G. and Mackensen, A.: Late Quaternary paleoproductivity and deep water circulation in the eastern South Atlantic Ocean: Evidence from benthic foraminifera, Palaeogeogr. Palaeoclimatol. Palaeoecol., 130(1–4), 43–80, doi:10.1016/S0031-0182(96)00137-X, 1997.

Schönfeld, J., Alve, E., Geslin, E., Jorissen, F., Korsun, S., Spezzaferri, S., Abramovich, S., Almogi-Labin, A., du Chatelet, E. A., Barras, C., Bergamin, L., Bicchi, E., Bouchet, V., Cearreta, A., Di Bella, L., Dijkstra, N., Disaro, S. T., Ferraro, L., Frontalini, F., Gennari, G., Golikova, E., Haynert, K., Hess, S., Husum, K., Martins, V., McGann, M., Oron, S., Romano, E.,

Sousa, S. M. and Tsujimoto, A.: The FOBIMO (FOraminiferal BIo-MOnitoring) initiative-Towards a standardised protocol for soft-bottom benthic foraminiferal monitoring studies, Mar. Micropaleontol., 94–95, doi:10.1016/j.marmicro.2012.06.001, 2012.

Schonfeld, J., Golikova, E., Korsun, S. and Spezzaferri, S.: The Helgoland Experiment - assessing the influence of methodologies on Recent benthic foraminiferal assemblage composition, J. Micropalaeontology, 32(2), 161–182, doi:10.1144/jmpaleo2012-022, 2013.

Seike, K., Shirai, K. and Kogure, Y.: Disturbance of Shallow Marine Soft-Bottom Environments and Megabenthos Assemblages by a Huge Tsunami Induced by the 2011 M9.0 Tohoku-Oki Earthquake, PLoS One, 8(6), doi:10.1371/journal.pone.0065417, 2013.

Takata, H., Lee, J.-M., Sakai, S., Nomura, R., Tsujimoto, A., Nishi, H., Lim, H. S. and Khim, B.-K.: Impact of early Oligocene deep water circulation to the benthic foraminifera in the eastern equatorial Pacific, Micropaleontology, 61(3), 2015.

Takayanagi, Y.: Manual of Microfossil Studies: Asakura Publishing, 161 p., 1978.

Tamura, T., Sawai, Y., Ikehara, K., Nakashima, R., Hara, J. and Kanai, Y.: Shallow-marine deposits associated with the 2011 Tohoku-oki tsunami in Sendai Bay, Japan, J. Quat. Sci., 30(4), 293–297, doi:10.1002/jqs.2786, 2015.

Thompson, P. R.: Foraminifers from deep sea drilling project Sites 434, 435, and 436, Japan Trench, Init. Rep. DSDP, 56/57, Pt. 2, 775–807, 1980.

Toyofuku, T., Duros, P., Fontanier, C., Mamo, B., Bichon, S., Buscail, R., Chabaud, G., Deflandre, B., Goubet, S., Gre'mare, A., Menniti, C., Fujii, M., Kawamura, K., Koho, K.A., Noda, A., Namegaya, Y., Oguri, K., Radakovitch, O., Murayama, M., Nooijer, L.J., Kurasawa, A., Ohkawara, N., Okutani, T., Sakaguchi, A., Jorissen, F., Reichart, G.-J., Kitazato, H.: Unexpected biotic resilience on the Japanese seafloor caused by the 2011 Tohoku-oki tsunami, Sci. Rep. http://dx.doi.org/10.1038/srep07517, 2014.

Tsuji, T., Kawamura, K., Kanamatsu, T., Kasaya, T., Fujikura, K., Ito, Y., Tsuru, T. and Kinoshita, M.: Extension of continental crust by anelastic deformation during the 2011 Tohoku-oki earthquake: The role of extensional faulting in the generation of a great tsunami, Earth Planet Sci. Lett., 364, 44–58, doi:10.1016/j.epsl.2012.12.038, 2013.

Tsujimoto, A., Nomura, R., Takata, H. and Kimoto, K.: A deep-sea benthic foraminiferal record of surface productivity changes during the constriction and closure of the Central American Seaway: IODP Hole U1338B, eastern equatorial Pacific, J. Foraminifer. Res., 43(4), doi:10.2113/gsjfr.43.4.361, 2013.

Tsujimoto, A., Nomura, R., Yasuhara, M. and Yoshikawa, S.: Benthic foraminiferal assemblages in Osaka Bay, southwestern Japan: faunal changes over the last 50 years, Paleontol. Res., 10(2), 141–161, doi:10.2517/prpsj.10.141, 2006.

Uchimura, H., Nishi, H., Takashima, R., Kuroyanagi, A., Yamamoto, Y. and Kutterolf, S.: Distribution of Recent Benthic Foraminifera off Western Costa Rica in the Eastern Equatorial Pacific Ocean, Paleontol. Res., 21(4), 380–396, doi:10.2517/2017PR003, 2017.

Urabe, J., Suzuki, T., Nishita, T. and Makino, W.: Immediate Ecological Impacts of the 2011 Tohoku Earthquake Tsunami on Intertidal Flat Communities, PLoS One, 8(5), doi:10.1371/journal.pone.0062779, 2013.

Usami, K., Ikehara, K., Jenkins, R. G. and Ashi, J.: Benthic foraminiferal evidence of deep-sea sediment transport by the 2011 Tohoku-oki earthquake and tsunami, Mar. Geol., 384, 214–224, doi:10.1016/j.margeo.2016.04.001, 2017.

Walton, W. R.: Techniques for recognition of living foraminifera. Contributions from the Cushman Foundation for Foraminiferal Research, 3, 56–60, 1952.

Yatsu, A., Chiba, S., Yamanaka, Y., Ito, S., Shimizu, Y., Kaeriyama, M. and Watanabe, Y.: Climate forcing and the Kuroshio / Oyashio ecosystem, 70(January), 922–933, 2013.

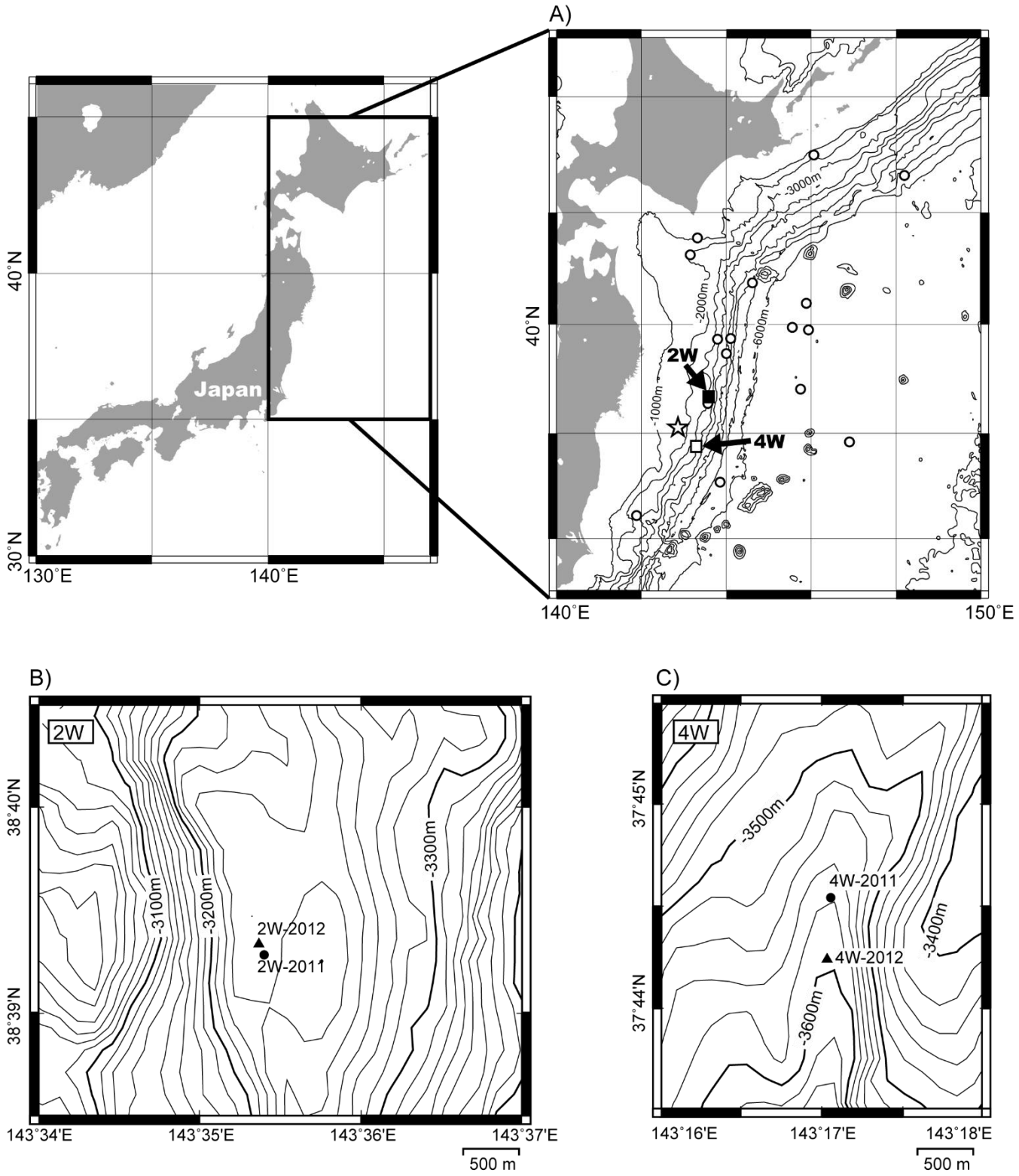

Fig. 1. Bathymetry of the studied area (A) and detailed sampling location of the sediment cores (B and C). The star symbol and open circles in figure 1-A indicate the epicenter of the 2011 Tohoku-oki earthquake and benthic foraminiferal samples used in Thompson (1980), respectively. Bathymetric map in figure 1-A was drawn by The Generic Mapping Tools (GMT) with bathymetric data from National Oceanic and Atmospheric Administration (NOAA).

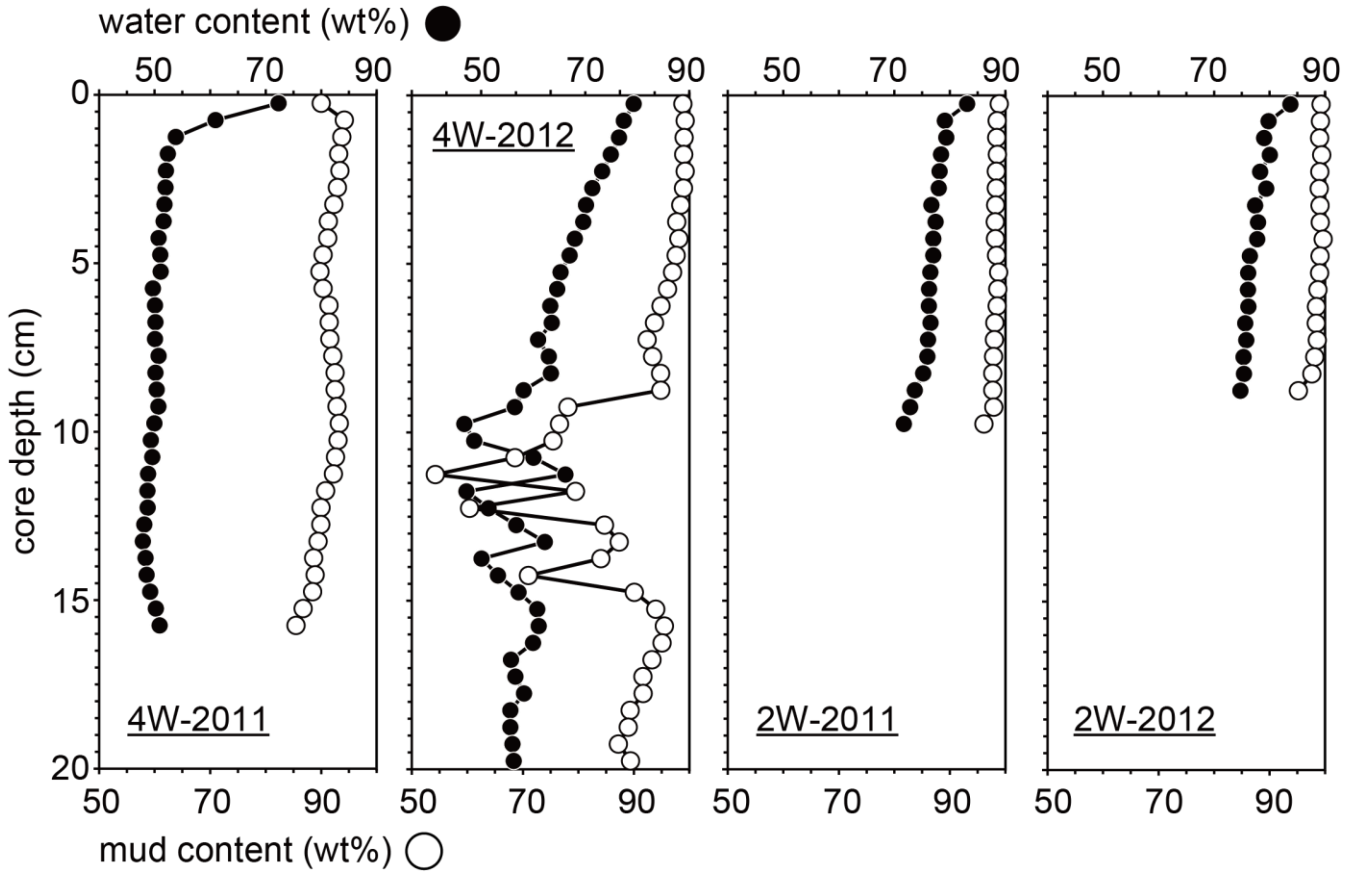

Fig. 2. Vertical profiles of water and mud contents in sediments.

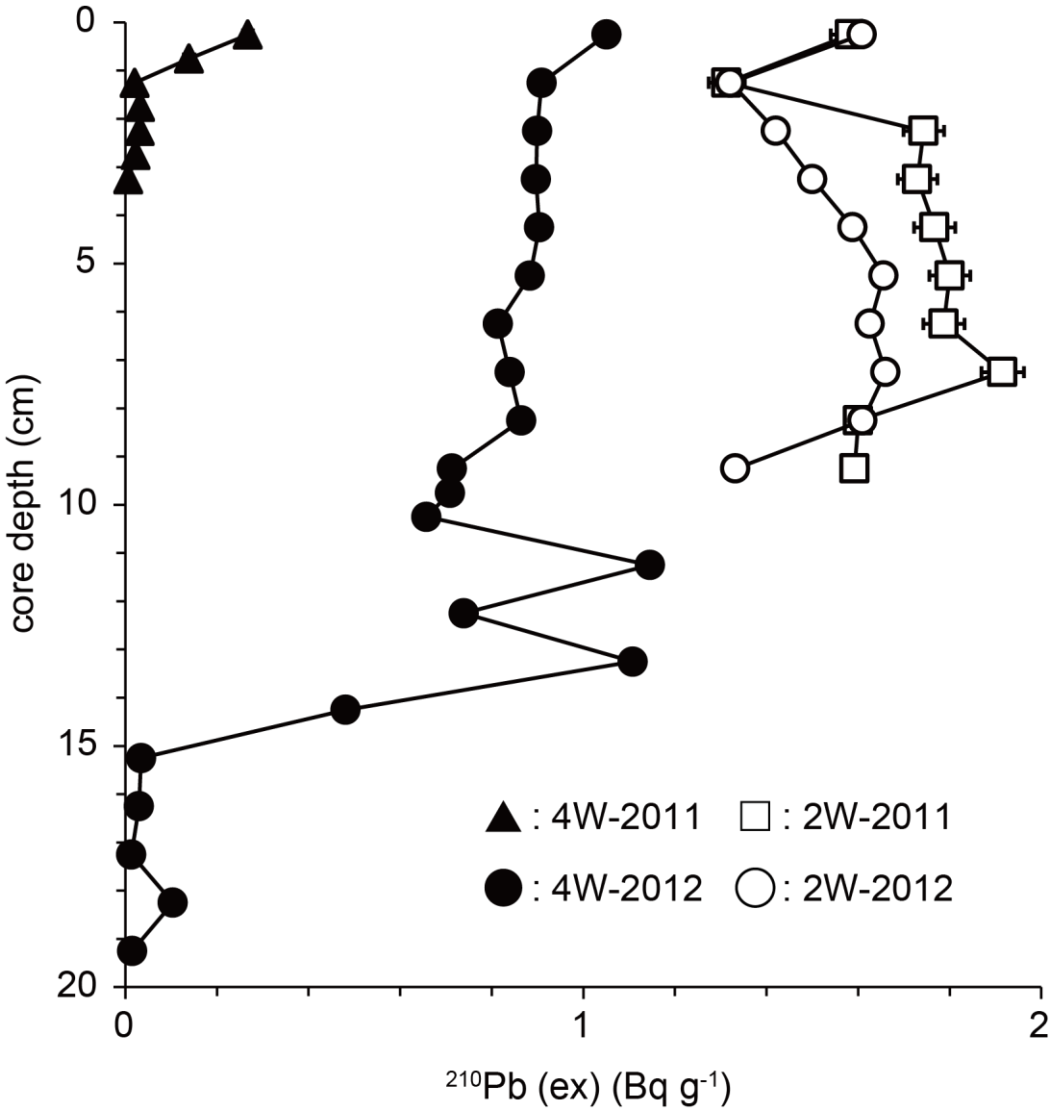

Fig. 3. Vertical profiles of the excess ^{210}Pbconcentrations decay-corrected to sampling date.

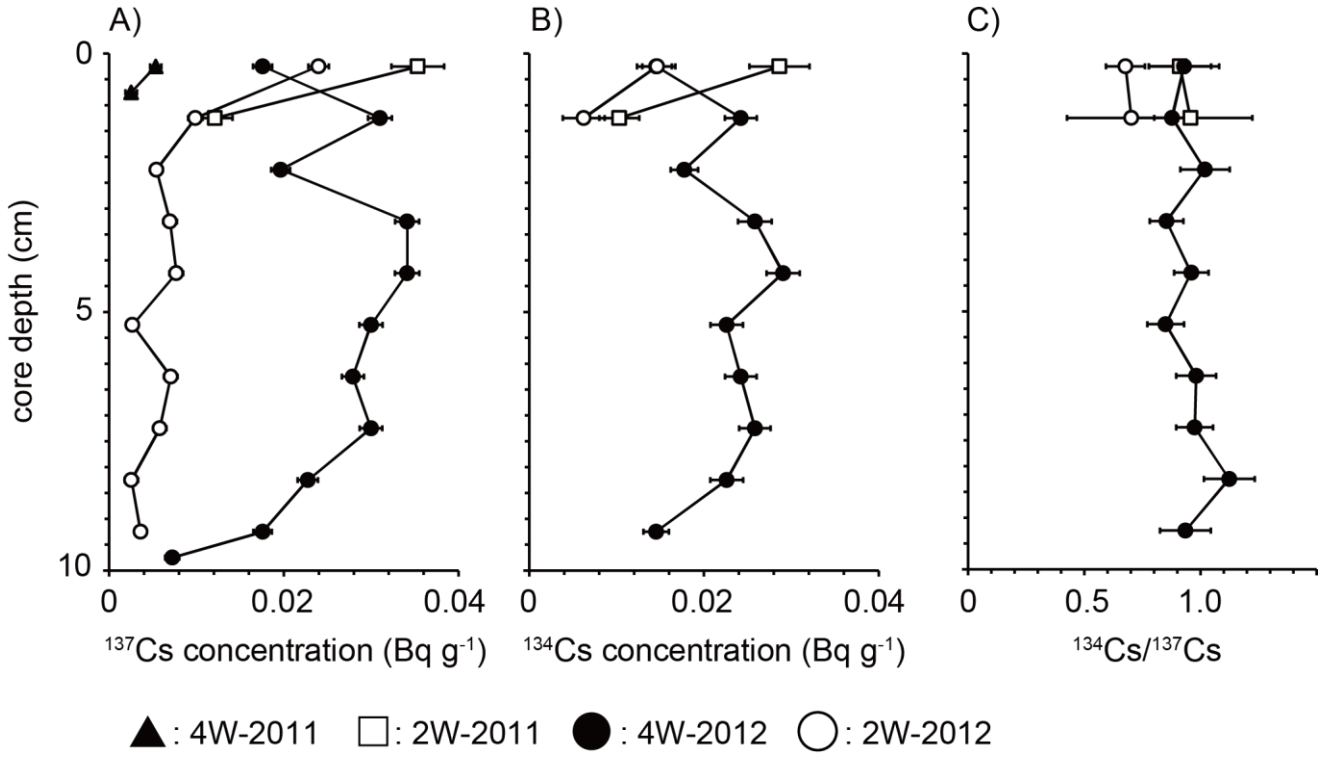

Fig. 4. Vertical profiles of A) ^{137}Cs concentrations decay-corrected to sampling date; B) ^{134}Cs concentrations decay-corrected to sampling date; C) ^{134}Cs/^{137}Cs ratio decay-corrected to the FNPP1 accident.

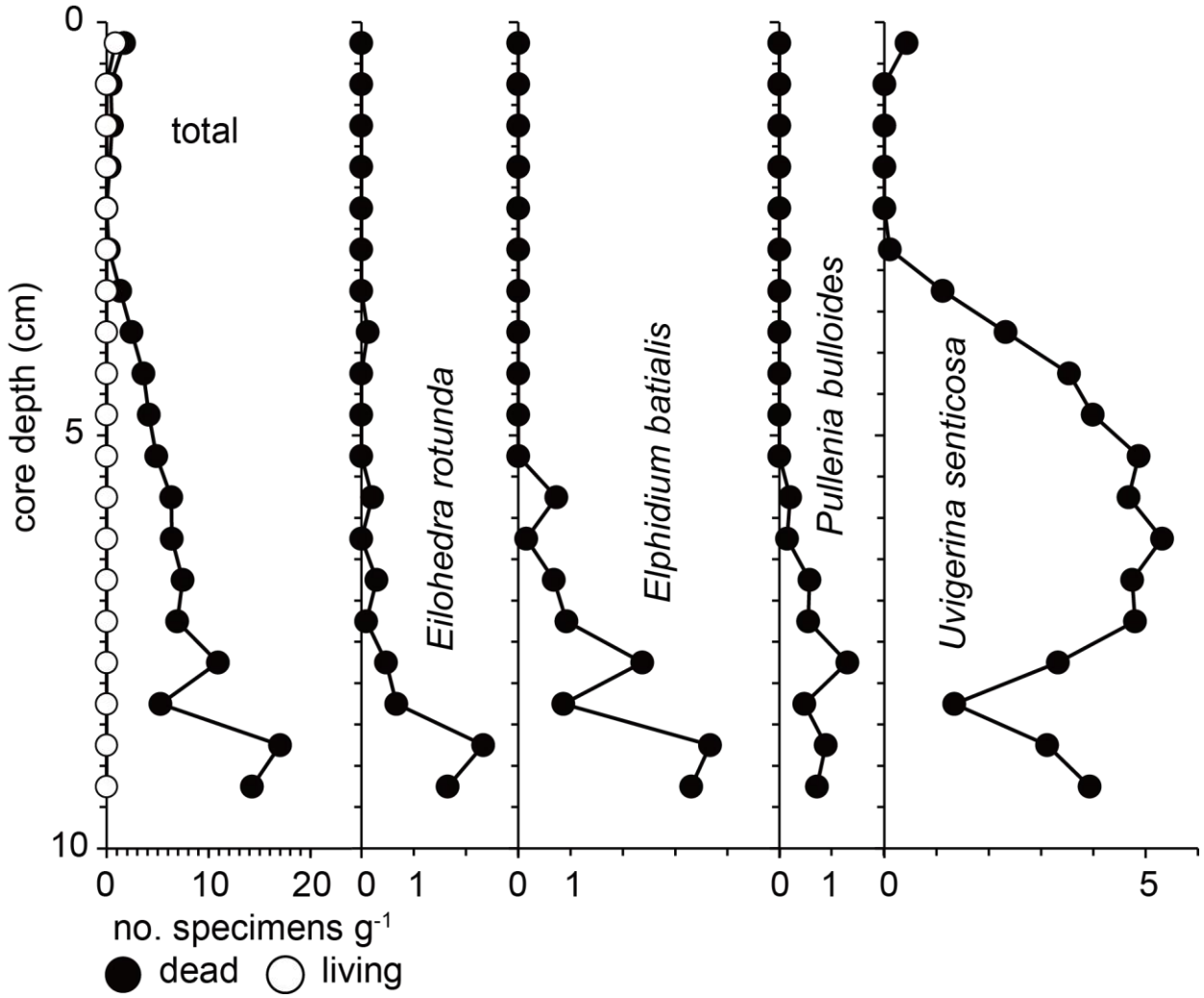

Fig. 5. Vertical distributions of absolute number of specimens per gram dry sediment of total foraminifera and dominant foraminiferal species in core 4W-2011. Open circles and filled circles indicate living (rose-Bengal stained) and dead foraminifera, respectively.

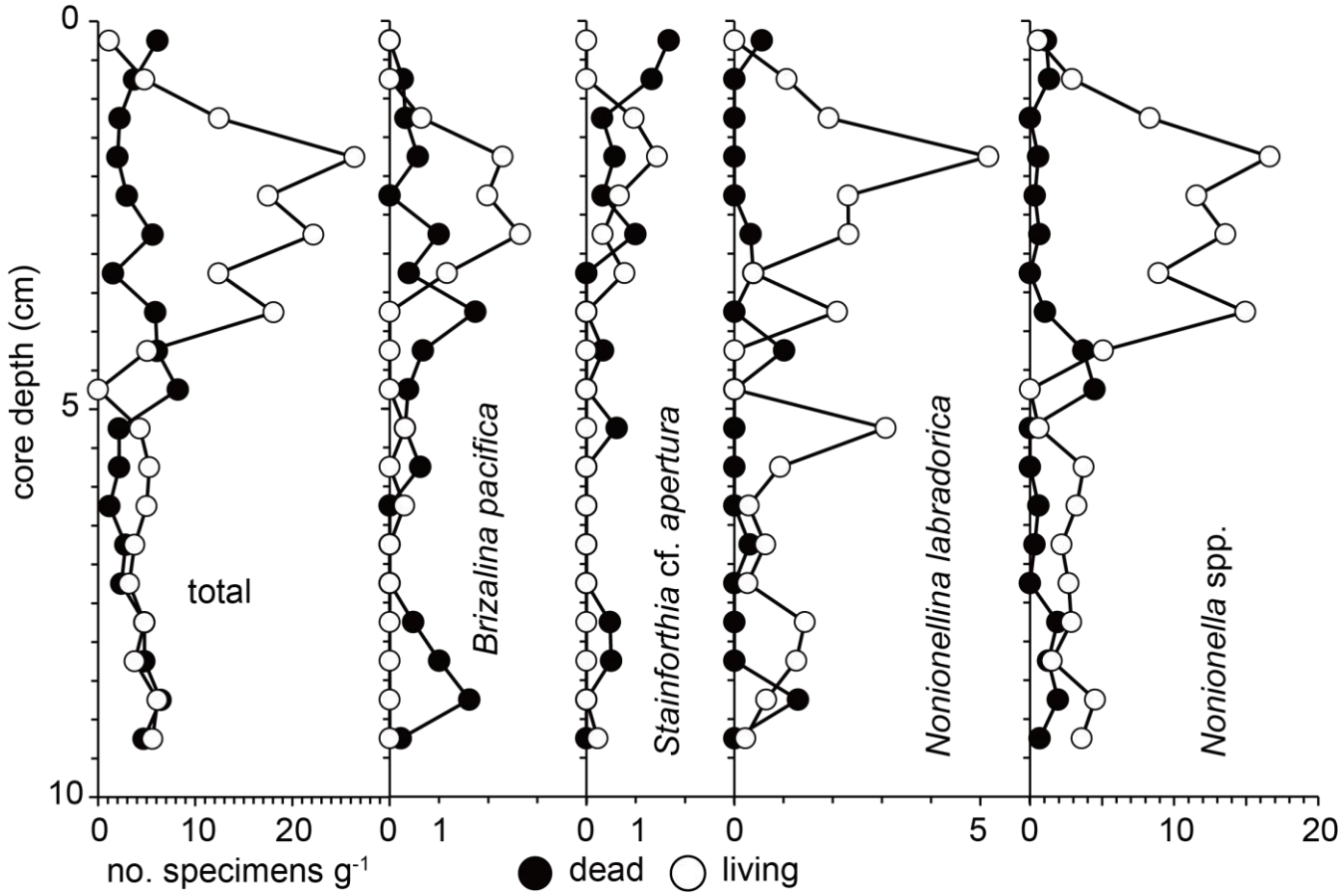

Fig. 6. Vertical distributions of absolute number of specimens per gram dry sediment of total foraminifera and dominant foraminiferal species in core 2W-2011. Open circles and filled circles indicate living (rose-Bengal stained) and dead foraminifera, respectively.

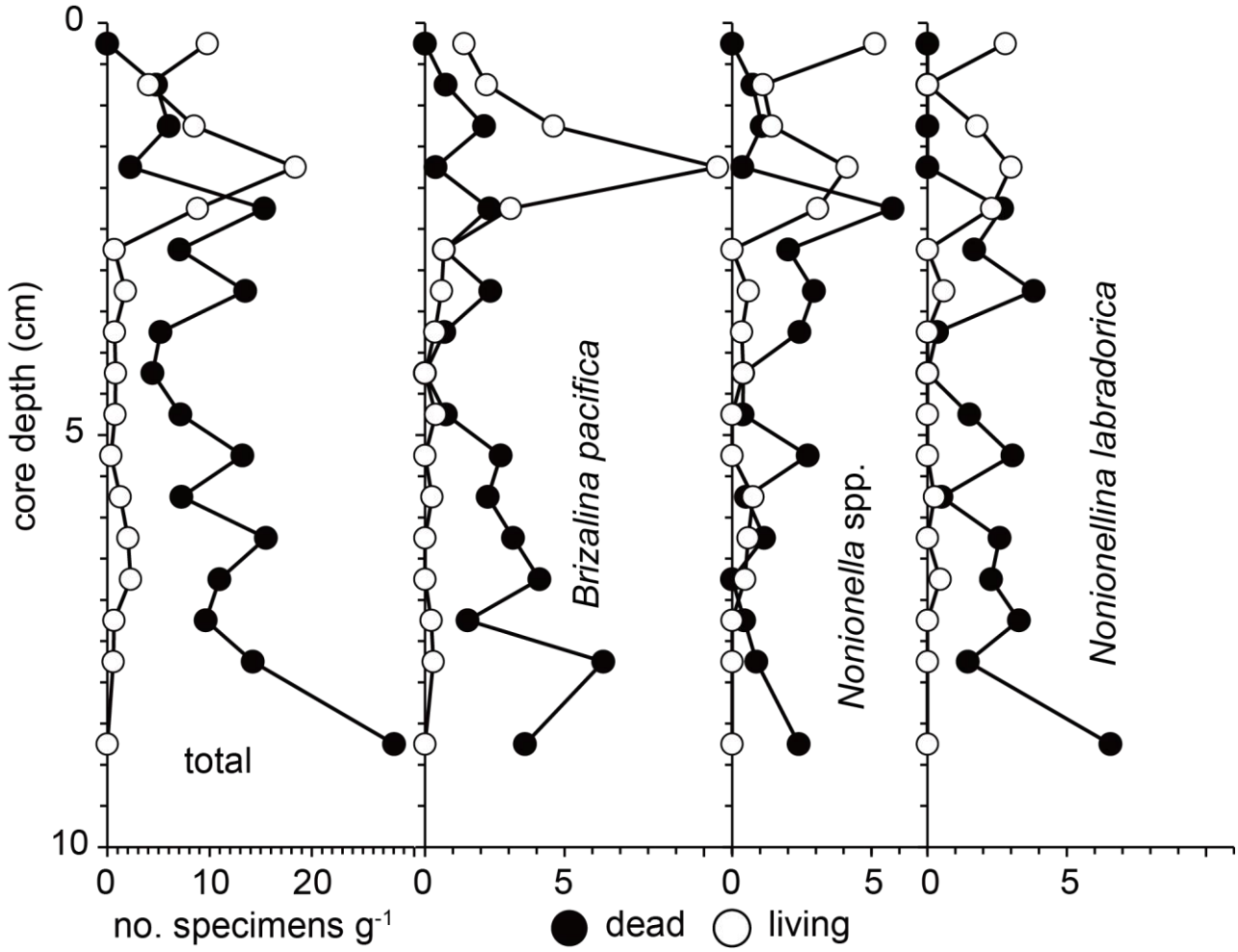

Fig. 7. Vertical distributions of absolute number of specimens per gram dry sediment of total foraminifera and dominant foraminiferal species in core 2W-2012. Open circles and filled circles indicate living (rose-Bengal stained) and dead foraminifera, respectively.

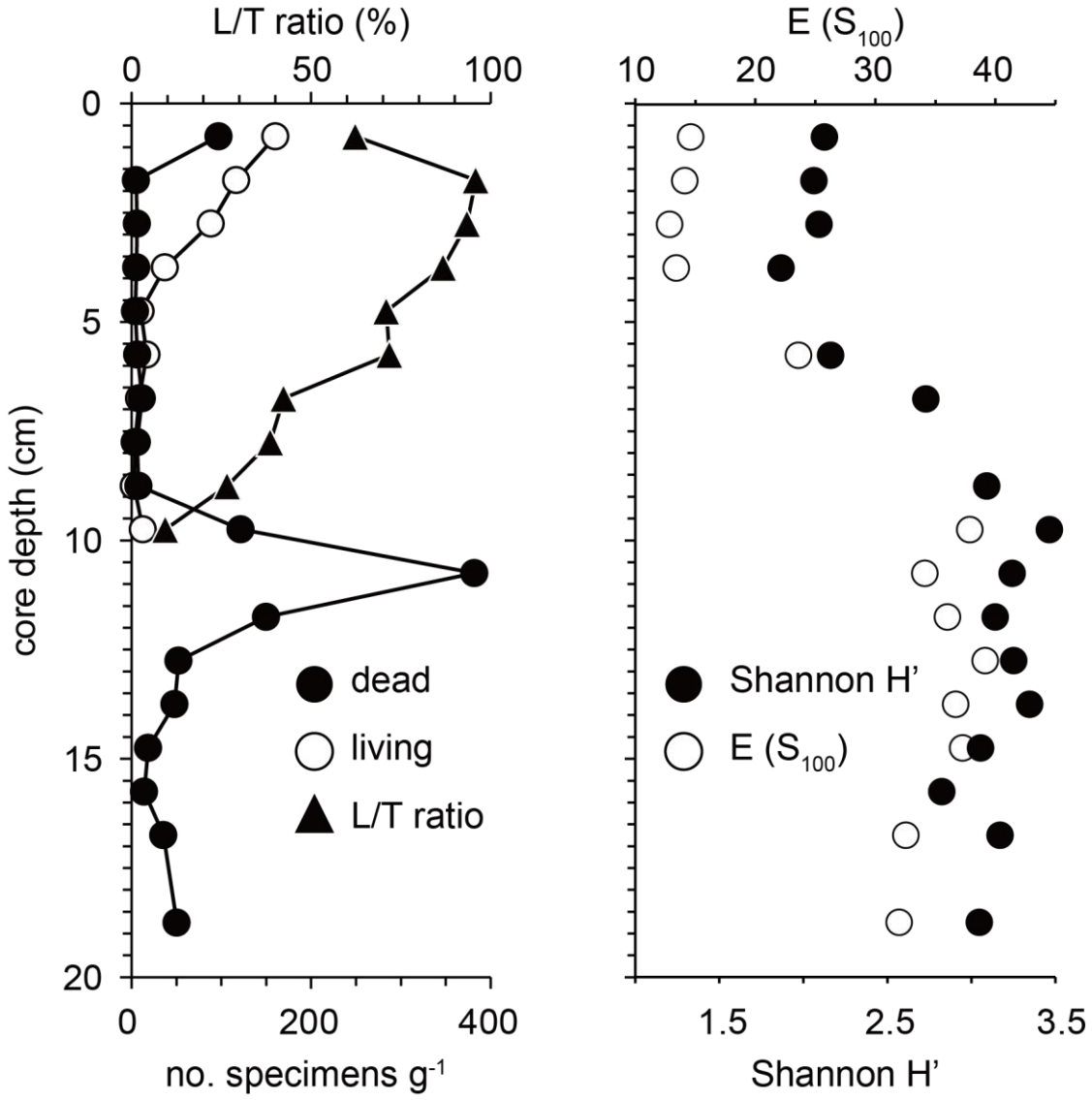

Fig. 8. Vertical profiles of dead and living foraminiferal density (ind. g^{-1}), and diversity index of total foraminiferal assemblage in core 4W-2012.

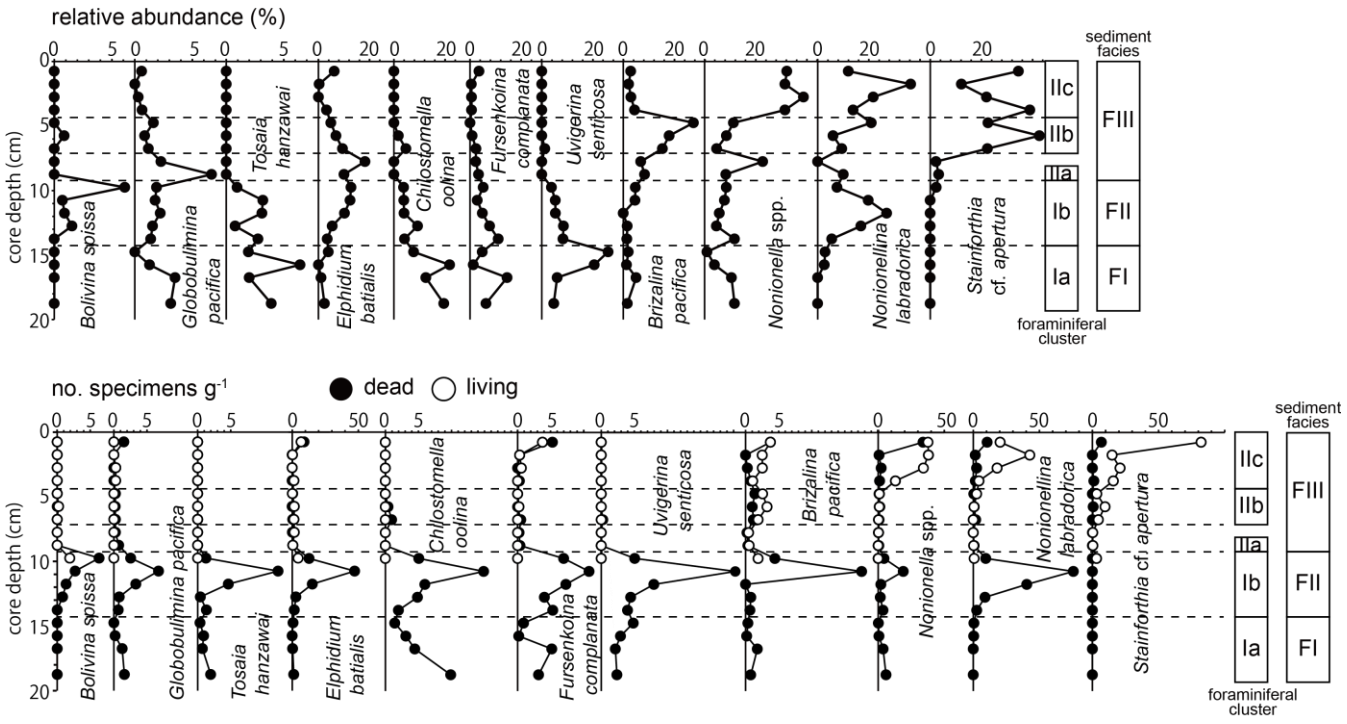

Fig. 9. Vertical distributions of relative and absolute number of specimens per gram dry sediment of dominant and characteristic foraminiferal species with Q-mode cluster grouping and sediment facies (FI, FII, and FIII) in core 4W-2012. Relative abundance is based on total (living and dead) assemblage. Open circles and filled circles for absolute number of specimens indicate living (rose-Bengal stained) and dead foraminifera, respectively.

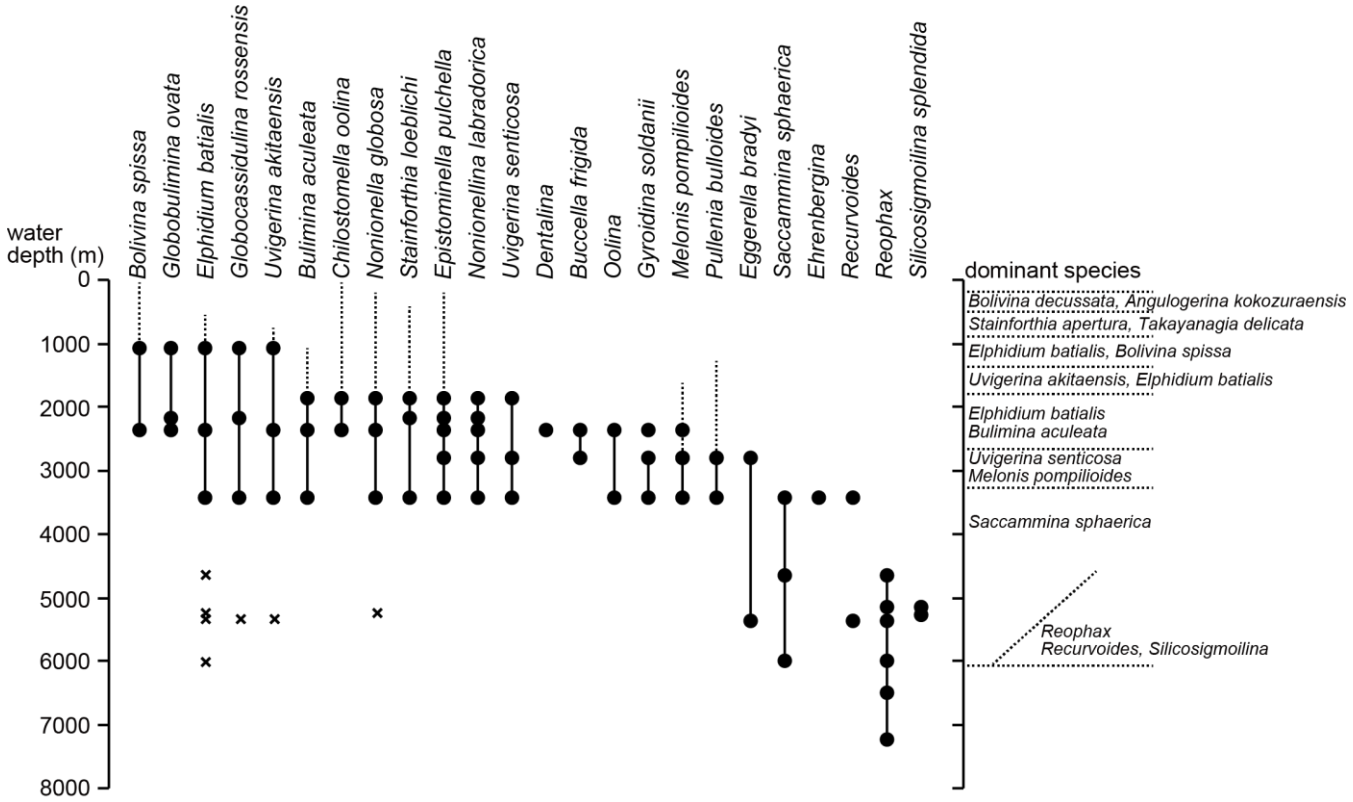

Fig. 10. Bathymetric distributions of benthic foraminiferal species in the Japan Trench area (modified after Thompson, 1980). The diagonal line in the abyssal dominant species indicate differences between west side and east side across the Japan Trench.

Table 1. Details of sampling sites of the sediment cores. *Station name used in Tsuji et al. (2013).

Core ID	Station*	Cruise ID	Submersible dive number	Sampling date	Latitude	Longtitude	Water depth (m)
4W-2011	4W	YK11-E06	1257	5 Aug 2011	37°44.54'N	143°17.06'E	3566
2W-2011	2W	YK11-E06	1259	10 Aug 2011	38°39.28'N	143°35.40'E	3230
4W-2012	4W	YK12-13	1310	18 Aug 2012	37°44.24'N	143°17.03'E	3585
2W-2012	2W	YK12-13	1312	21 Aug 2012	38°39.34'N	143°35.37'E	3230

Table 2. γ-Spectrometry results of the sediment samples examined. Error indicates a standard deviation of counting statistics. *Concentrations decay-corrected based on sampling date. **Concentrations decay-corrected based on date of the FNPP1 accident. The "b.d.l." denotes "below detection limit".

	mean depth (cm)	excess ^{210}Pb* (Bq g^{-1})	^{137}Cs* (Bq g^{-1})	^{134}Cs * (Bq g^{-1})	^{134}Cs /^{137}Cs**
4W-2011	0.25	0.268 ± 0.011	0.005 ± 0.001	b.d.l.	---
	0.75	0.139 ± 0.011	0.003 ± 0.001	b.d.l.	---
	1.25	0.021 ± 0.006	b.d.l.	b.d.l.	---
	1.75	0.032 ± 0.006	b.d.l.	b.d.l.	---
	2.25	0.032 ± 0.007	b.d.l.	b.d.l.	---
	2.75	0.023 ± 0.007	b.d.l.	b.d.l.	---
	3.25	0.006 ± 0.007	b.d.l.	b.d.l.	---
2W-2011	0.25	1.583 ± 0.042	0.035 ± 0.003	0.029 ± 0.003	0.91 ± 0.13
	1.25	1.313 ± 0.039	0.012 ± 0.002	0.010 ± 0.002	0.96 ± 0.27
	2.25	1.743 ± 0.044	b.d.l.	b.d.l.	---
	3.25	1.730 ± 0.043	b.d.l.	b.d.l.	---
	4.25	1.767 ± 0.045	b.d.l.	b.d.l.	---
	5.25	1.801 ± 0.045	b.d.l.	b.d.l.	---
	6.25	1.787 ± 0.045	b.d.l.	b.d.l.	---
	7.25	1.916 ± 0.046	b.d.l.	b.d.l.	---
	8.25	1.601 ± 0.023	b.d.l.	b.d.l.	---
	9.25	1.593 ± 0.023	b.d.l.	b.d.l.	---
4W-2012	0.25	1.098 ± 0.022	0.018 ± 0.001	0.015 ± 0.002	0.93 ± 0.15
	1.25	0.950 ± 0.019	0.031 ± 0.001	0.024 ± 0.002	0.88 ± 0.08
	2.25	0.940 ± 0.021	0.020 ± 0.001	0.018 ± 0.002	1.02 ± 0.11
	3.25	0.938 ± 0.021	0.034 ± 0.001	0.026 ± 0.002	0.85 ± 0.07
	4.25	0.945 ± 0.021	0.034 ± 0.001	0.029 ± 0.002	0.96 ± 0.07
	5.25	0.924 ± 0.021	0.030 ± 0.001	0.023 ± 0.002	0.85 ± 0.08
	6.25	0.851 ± 0.020	0.028 ± 0.001	0.024 ± 0.002	0.98 ± 0.09
	7.25	0.877 ± 0.020	0.030 ± 0.001	0.026 ± 0.002	0.97 ± 0.08
	8.25	0.904 ± 0.020	0.023 ± 0.001	0.023 ± 0.002	1.12 ± 0.11
	9.25	0.746 ± 0.019	0.018 ± 0.001	0.015 ± 0.001	0.94 ± 0.11
	9.75	0.741 ± 0.019	0.007 ± 0.001	b.d.l.	---
2W-2012	0.25	1.609 ± 0.024	0.024 ± 0.001	0.015 ± 0.002	0.68 ± 0.08
	1.25	1.322 ± 0.022	0.010 ± 0.001	0.006 ± 0.002	0.70 ± 0.28
	2.25	1.421 ± 0.023	0.005 ± 0.001	b.d.l.	---
	3.25	1.501 ± 0.023	0.007 ± 0.001	b.d.l.	---
	4.25	1.589 ± 0.024	0.008 ± 0.001	b.d.l.	---
	5.25	1.656 ± 0.024	0.003 ± 0.001	b.d.l.	---
	6.25	1.626 ± 0.024	0.007 ± 0.001	b.d.l.	---
	7.25	1.660 ± 0.024	0.006 ± 0.001	b.d.l.	---
	8.25	1.610 ± 0.024	0.003 ± 0.001	b.d.l.	---
	9.25	1.333 ± 0.022	0.004 ± 0.001	b.d.l.	---

Supplementary figures

Figure S1. Scanning Electron Microscope (SEM) images of dominant and characteristic species.

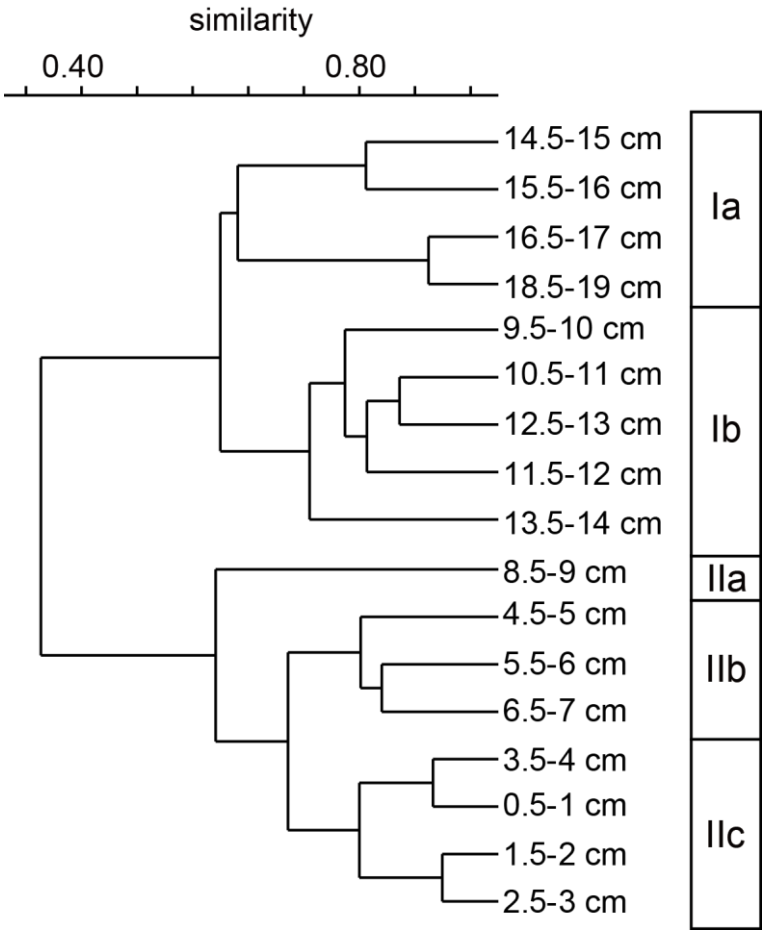

Figure S2. Dendrogram of Q-mode cluster analysis of 4W-2012 core.

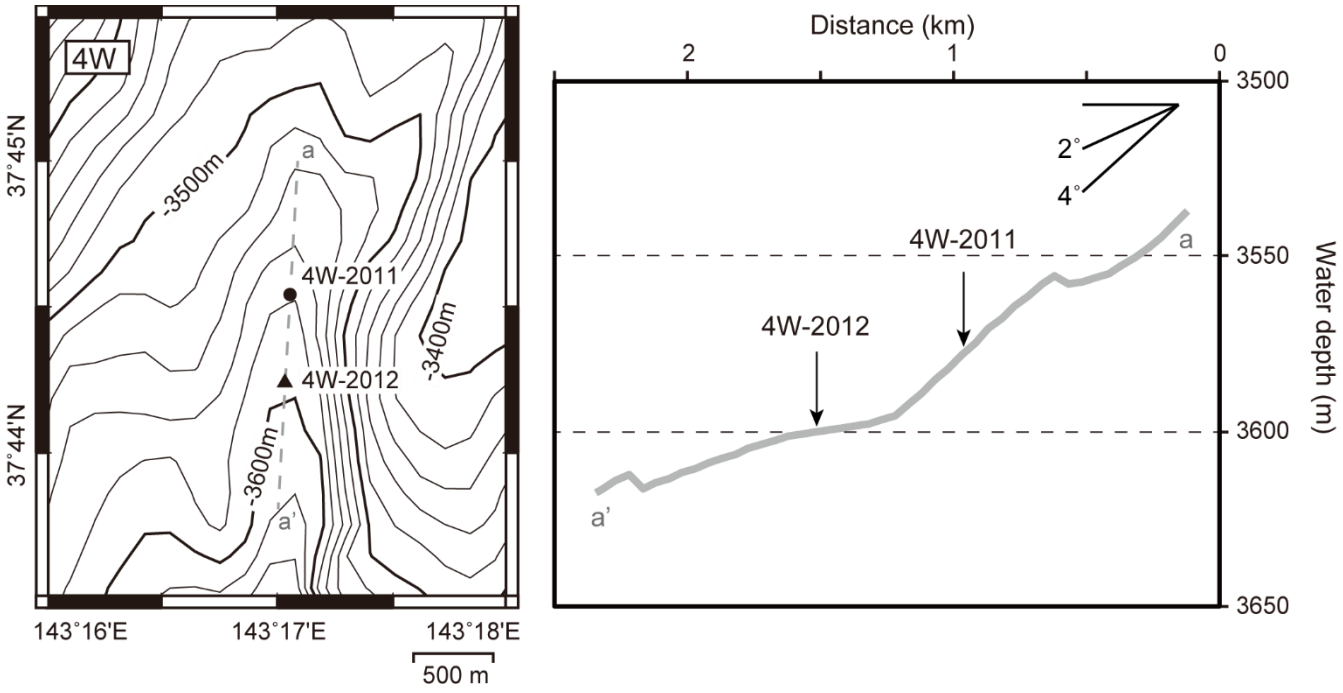

Figure S3. Bathymetric map of site 4W (left) and bathymetric profile (right) along the gray dash line in left figure (same map to Figure 1C).

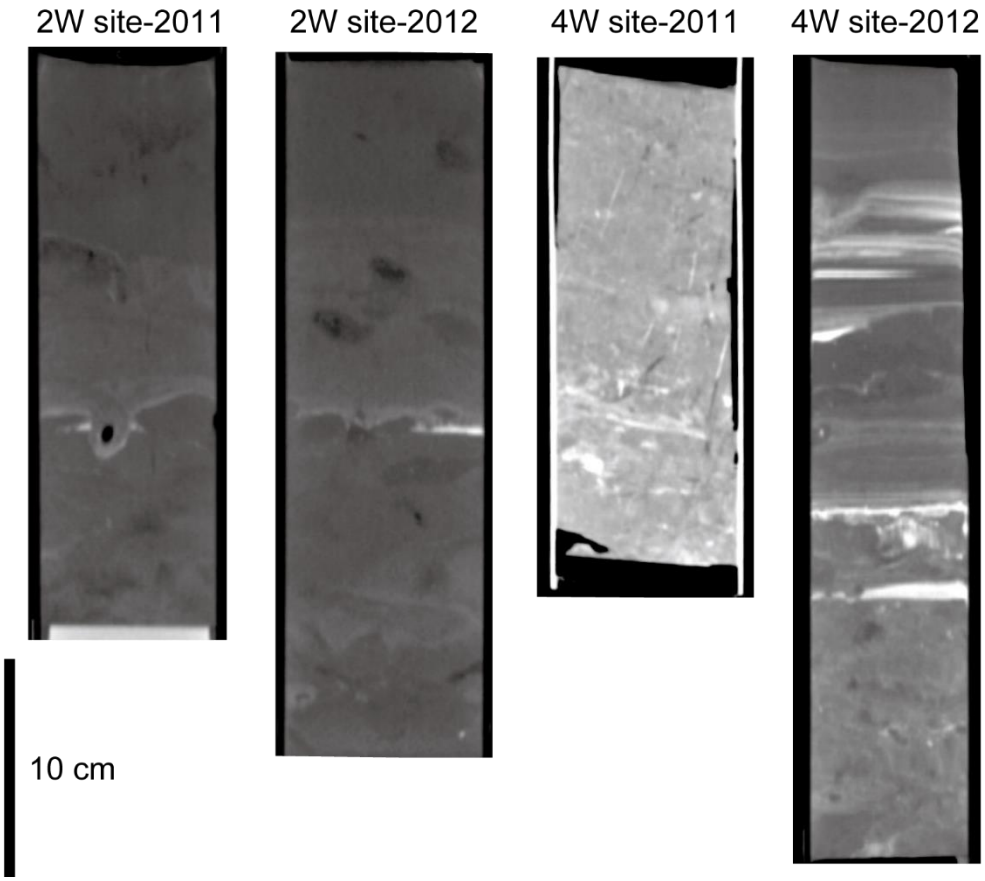

Figure S4. X-ray CT reslice images (Window Level 650, Window Width 1000) of cores for sedimentological analysis collected at same sites to foraminiferal cores within a few meters. The X-ray CT scanning was performed on HITACHI X-ray CT unit (RADIX-PRATICO, FR version, Hitachi Medical Corporation) in the Center for Advanced Marine Core Research, Kochi University.

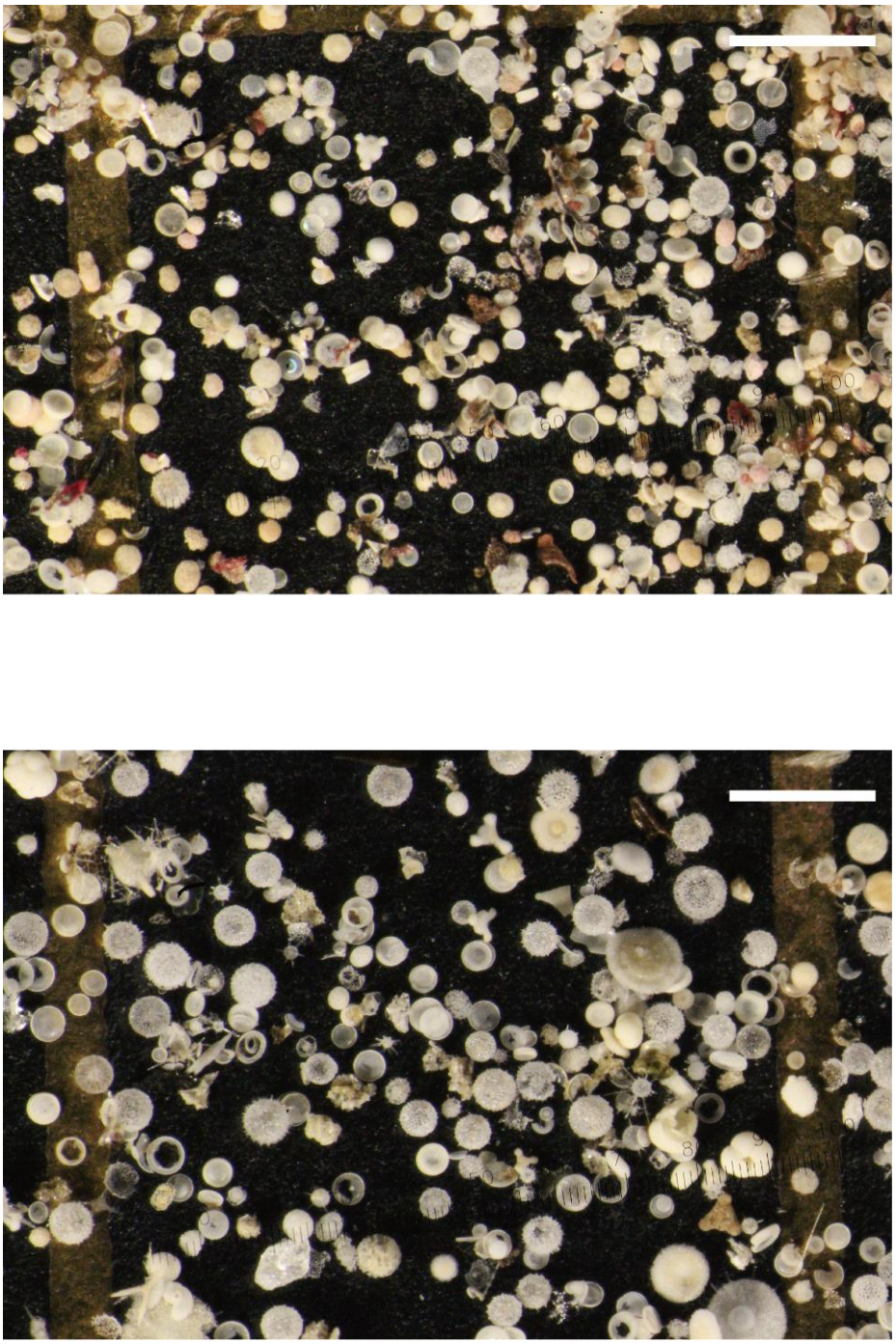

Figure S5. Images of the >106-µm fraction taken with a digital single-lens reflex camera through stereoscopic microscope at 4.5-5.0 cm (upper image) and 15.5-16.0 cm (lower image) of 4W-2012 core. White bars = 1 mm

Title for supplementary table

Table S1. Foraminiferal species identified in this study.

Table S2. Total organic carbon concentration (TOC), total nitrogen (TN) concentrations, C/N ratio (weight ratio), carbon isotopic compositions, and nitrogen isotopic compositions of the core collected some tens cm away from 4W-2012 core. Sample preparations and measurements followed Nomaki et al. (2016b).

Depth in sediments (cm)	TOC (wt %)	TN (wt %)	C/N (wt/wt)	$d^{13}C$ (‰)	$d^{15}N$ (‰)
0.25	4.5	0.58	7.7	-21.1	5.2
0.75	4.7	0.61	7.8	-21.0	5.1
1.25	4.5	0.57	7.8	-21.1	5.5
1.75	4.6	0.59	7.8	-21.1	5.2
2.25	3.7	0.48	7.8	-21.0	5.0
2.75	3.3	0.43	7.8	-21.0	4.9
3.5	4.5	0.58	7.7	-21.0	5.1
4.5	4.1	0.52	7.8	-21.2	5.0
5.5	4.1	0.53	7.8	-21.0	5.3
7.5	3.9	0.49	7.9	-21.0	5.2
10.5	4.1	0.52	7.9	-21.1	5.3